Appendix A.12:

Avondale Playground – VsVp 57062

Table 1: Site Description for Avondale Playground (v_Sv_P 57062).

Attribute	Yes/No			Description/Date	Symbol in Figure 1
	10-m Buffer	20-m Buffer	50-m Buffer		
Near a body of surface water or other free face features?	No	No	No	The center of the site is 350 meters away from the Avon River.	NA
Lateral spreading observed during the CES?	No	No	No	Ground cracks indicating lateral spreading were not observed by the mapping team.[1]	NA
Nearby buildings or structures?	Yes	Yes	Yes	Residential buildings cover 1% of the 10-m buffer (the NW quadrant), 11% of the 20-m buffer (the NW and NE quadrants) and 21% of the 50-m buffer (the NE, NW, and SW quadrants).	White Fill + Brown Outline
Sloping land?	No	No	No	NA	NA
Step changes in the ground surface?	No	No	No	NA	NA
Retaining walls?	No	No	No	NA	NA
Vegetation?	Yes	Yes	Yes	Trees cover 4% of the 10-m buffer (the NW quadrant), while trees and bushes cover 11% of the 20-m buffer (the NE, NW, and SW quadrants) and 20% of the 50-m buffer (all quadrants).	White Fill + Green Outline
Anthropogenic changes to the site between the LiDAR surveys?	Yes	Yes	Yes	Removal of a dwelling (Avondale Rd 70) sometime between Jan 2013 and Mar 2013. Addition of a building on the same property sometime between Sep 2013 and Feb 2014. During the same time, another dwelling (Niven St 34) was removed. Earthwork was performed on this property between Mar 2014 and Sep 2014 and a new dwelling was built sometime between Apr 2015 and July 2015. Earthwork was also done in the park sometime after Apr 2012 as part of remediation.	Brown X Sign
Other important factors?	Yes	Yes	Yes	Road covers 3% of the 50-m buffer. Playground with equipment is situated in the SE quadrant, affecting the 50-m buffer only; it covers 4% of the area.	Road: White Fill + Gray Outline; Playground: White Fill + Yellow Outline

Notes: Buffer is the area within a circle of a specified radius with VsVp investigations done at its center (172.687194°, -43.508109°); the Oct-15 LiDAR survey will not be used for the analysis due to the anthropogenic changes.

[1] Canterbury Geotechnical Database. (2012). "Observed Ground Crack Locations", Map Layer CGD0400 - 23 July 2012, retrieved July 09, 2018 from https://canterburygeotechnicaldatabase.projectorbit.com/

Figure 1: Site plan with areas where LiDAR survey data is considered.

Note 1: The area in the free-field selected for settlement assessment is level, free of vegetation and structures, and without anthropogenic changes from July 2003 to Feb 2012, all of which have the potential to affect the LiDAR-based settlement estimates.

Table 2: LiDAR flight error adjustments, global adjustments for the difference between average LiDAR point elevations and benchmark survey elevations, and vertical tectonic movement adjustments.

	Adjustments (mm)		
Earthquake Event(s)	LiDAR Flight Error	Global Offset[2]	Tectonic Vertical Movement
Sep-10	0	-3	0
Feb-11	0	16	-40
Jun-11	0	38	-45
Dec-11	-50	-65	-5
CES	-50	-14	-90
Any LiDAR survey affected by ejecta?*			Yes

Notes: The negative sign indicates the subtraction from the ground surface subsidence, while the positive sign indicates the addition to the ground surface subsidence; * indicates that ejecta were present at the site during all post Feb-11 LiDAR surveys (except the Oct-15 LiDAR survey prior to which the earthwork was done at the site) hence 50, 40, and 15 mm of ground surface subsidence (based on physical evidence) for the 10-, 20- and 50-m buffers, respectively, are added for the Feb-11 EQ and the CES.

Table 3: LiDAR Measurement Error.

Surveys	Buffer	Area Averaged Difference Indicating Repeat Measurement Error (mm)	$\sigma^*_{\text{individual LiDAR points}}$ (mm)	%Reduction in σ due to Area Averaging of LiDAR Points
Post Feb 2011: Mar 2011 and May 2011	10-m	118	59	[78,200]
	20-m	46		
	50-m	52		
Post Dec 2011: Feb 2012 and Oct 2015**	10-m	NA	70	[NA,NA]
	20-m	NA		
	50-m	NA		

*Standard deviation; ** indicates that the difference in the ground surface elevation was not assessed due to the site remediation following the Feb-12 LiDAR survey.

[2] Russell, J., & van Ballegooy, S. (2015). *Canterbury Earthquake Sequence: Increased liquefaction vulnerability assessment methodology*. New Zealand: Tonkin & Taylor Ltd.

Table 4: Ground surface subsidence adjustments due to LiDAR measurement error.

Earthquake Event(s)	$\sigma_{\text{pre-EQ LiDAR survey}}$ (mm)	$\sigma_{\text{post-EQ LiDAR survey}}$ (mm)	σ_{total} (mm)	Area Average Adjusted σ (mm) **
Sep-10	158	56	134	±268
Feb-11	56	59	59	±118
Jun-11	59	61	62	±124
Dec-11	61	70	87	±173
CES	158	70	124	±249

**Based on the highest %Reduction in Table 3.

Table 5: Raw liquefaction-related ground surface subsidence using original LiDAR points.

	Average Ground Surface Subsidence (mm)		
Earthquake Event(s)	10-m Buffer	20-m Buffer	50-m Buffer
Sep-10	22	18	24
Feb-11	135	145	160
Jun-11	83	85	86
Dec-11	87	87	68
CES	327	335	338

Table 6: Corrected liquefaction-related ground surface subsidence using original LiDAR points with the calculated adjustments in Table 2.

	Average Calculated Ground Surface Subsidence (mm)		
Earthquake Event(s)	10-m Buffer	20-m Buffer	50-m Buffer
Sep-10	19±275	15±275	21±275
Feb-11	161±125	161±125	151±125
Jun-11	76±125	78±125	79±125
Dec-11	-33±175	-33±175	-52±175
CES	223±250	221±250	199±250

Notes: Plus/minus values are same as those in Table 4, but rounded to the nearest 25; Positive overall values indicate ground surface subsidence, while negative overall values indicate ground surface uplift.

Table 7: Corrected liquefaction-related ground surface subsidence using LiDAR DEMs.

	Estimated Ground Surface Subsidence (mm)								
	10-m Buffer			20-m Buffer			50-m Buffer		
Earthquake Event(s)	16th %ile	50th %ile	84th %ile	16th %ile	50th %ile	84th %ile	16th %ile	50th %ile	84th %ile
Sep-10	50	50	50	50	50	50	50	50	50
Feb-11	150	150	150	150	150	150	150	150	150
Jun-11	50	50	50	50	50	50	50	50	50
Dec-11	<50	50	100	<50	50	100	<50	<50	100
CES	300	300	300	200	300	300	200	200	300

Note: These percentiles are not the exact statistical measures; they indicate the spatial variability of ground surface subsidence.

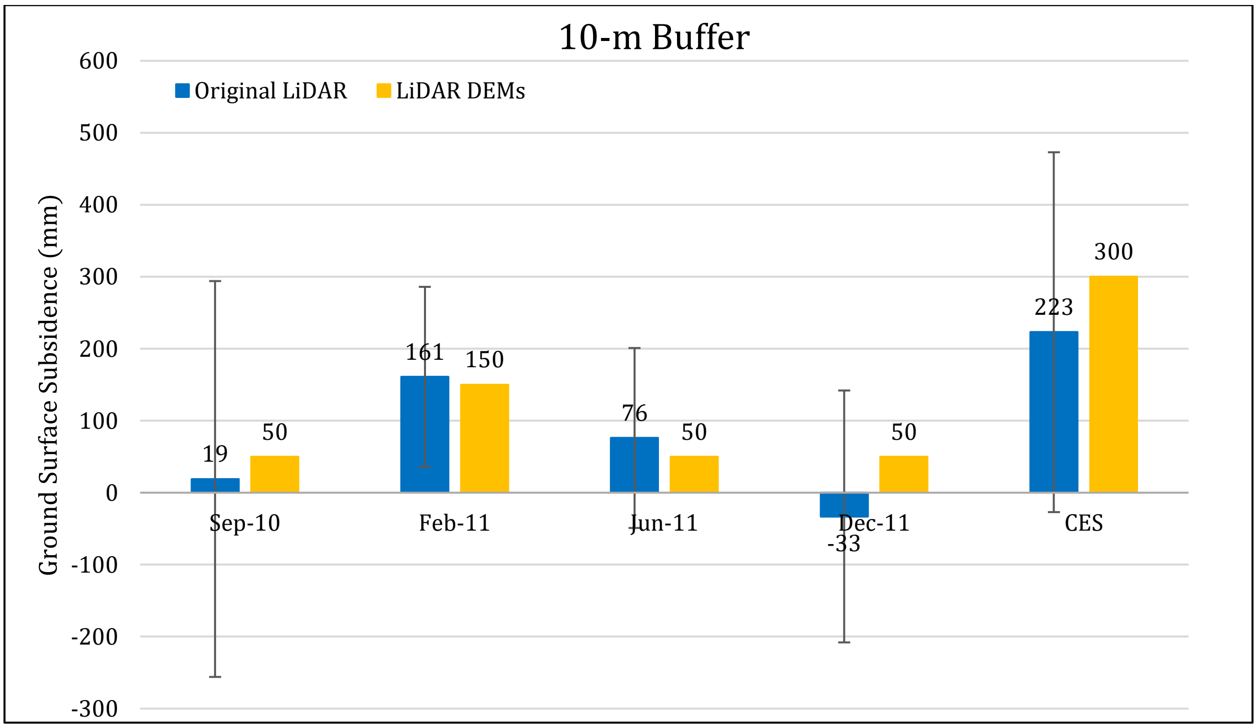

Figure 2: Comparison between ground surface subsidence determined from original LiDAR survey points and ground surface subsidence (50th %ile) estimated using LiDAR DEMs for the 10-m buffer.

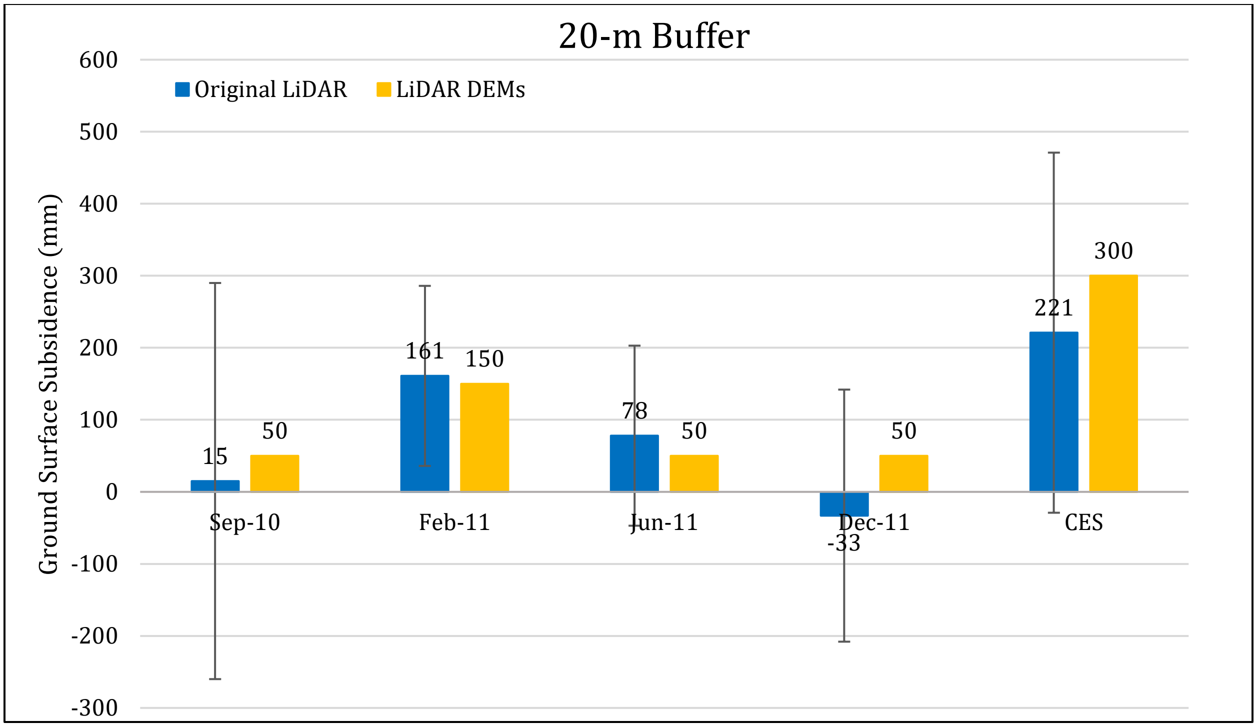

Figure 3: Comparison between ground surface subsidence determined from original LiDAR survey points and ground surface subsidence (50th %ile) estimated using LiDAR DEMs for the 20-m buffer.

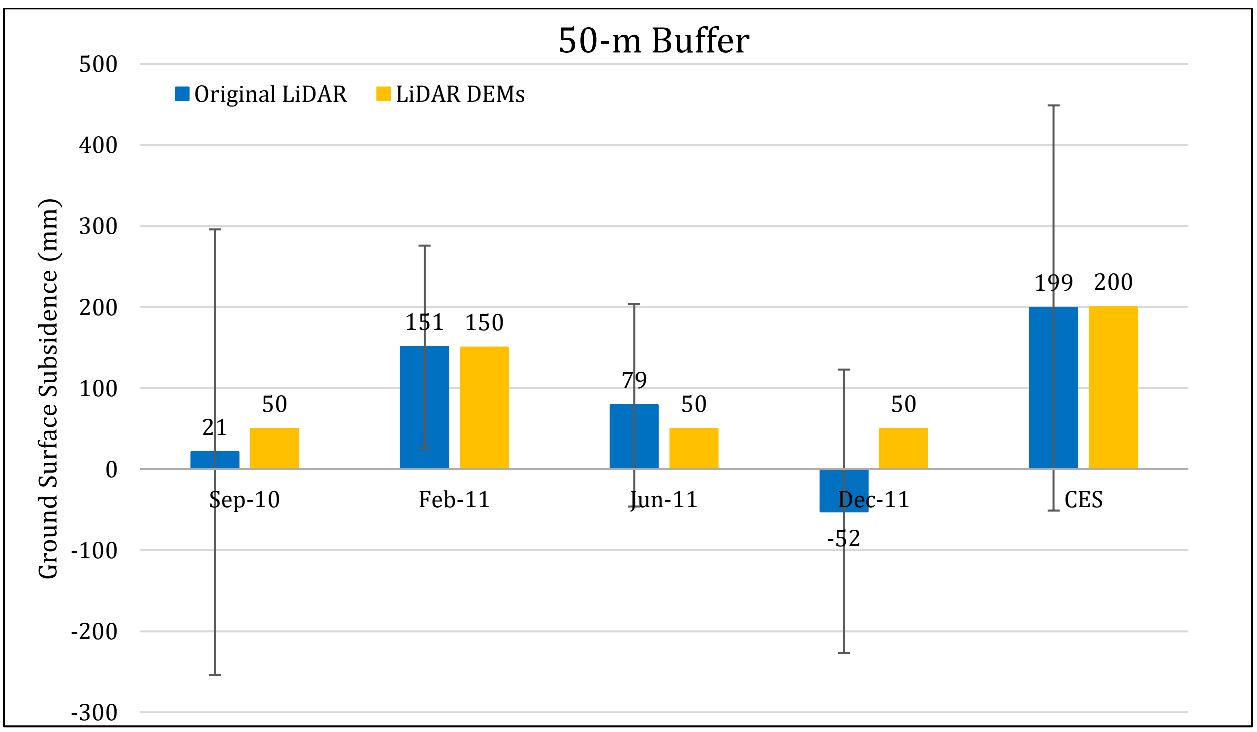

Figure 4: Comparison between ground surface subsidence determined from original LiDAR survey points and ground surface subsidence (50th %ile) estimated using LiDAR DEMs for the 50-m buffer.

Note 2: The ground surface subsidence values determined from original LiDAR survey points are generally similar to the ground surface subsidence values estimated using LiDAR DEMs for all earthquake events.

Table 8a: Ejecta-Induced settlement for the top 20 m of the soil profile for the 10-m buffer for the 50th %ile PGA, P_L=50%, and C_{FC}=0.13 using BI-2014, ZRB-2002, and I_C cutoff of 2.6.

Earthquake Event(s)	M_W	PGA (g)	Depth to Groundwater (m)	S_T (mm)	S_{V1D} (mm)	$S_{E,L}$ (mm)
Sep-10	7.1	0.18	2.1	19±275	7±20	12±276
Feb-11	6.2	0.40	2.2	161±125	93±50	68±135
Jun-11	6.2	0.26	1.9	76±125	32±25	44±128
Dec-11	6.1	0.30	2.6	-33±175	30±50	-63±182

Notes: S_T = Total settlement (Table 6); S_{V1D} = Average vertical settlement due to volumetric compression using Boulanger and Idriss (2014) (BI-2014), Zhang et al. (2002) (ZRB-2002) procedures and de Greef and Lengkeek (2018) thin-layer correction; $S_{E,L}$ = Ejecta-induced settlement as the difference between the LiDAR-based S_T and S_{V1D}.

Table 8b: Ejecta-Induced settlement for the top 20 m of the soil profile for the 20-m buffer for the 50th %ile PGA, P_L=50%, and C_{FC}=0.13 using BI-2014, ZRB-2002, and I_C cutoff of 2.6.

Earthquake Event(s)	M_W	PGA (g)	Depth to Groundwater (m)	S_T(mm)	S_{V1D} (mm)	$S_{E,L}$ (mm)
Sep-10	7.1	0.18	2.1	15±275	13±20	2±276
Feb-11	6.2	0.40	2.2	161±125	112±50	49±135
Jun-11	6.2	0.26	1.9	78±125	44±25	34±128
Dec-11	6.1	0.30	2.6	-33±175	46±50	-79±182

Notes: S_T = Total settlement (Table 6); S_{V1D} = Average vertical settlement due to volumetric compression using Boulanger and Idriss (2014) (BI-2014), Zhang et al. (2002) (ZRB-2002) procedures and de Greef and Lengkeek (2018) thin-layer correction; $S_{E,L}$ = Ejecta-induced settlement as the difference between the LiDAR-based S_T and S_{V1D}.

Table 8c: Ejecta-Induced settlement for the top 20 m of the soil profile for the 50-m buffer for the 50th %ile PGA, P_L=50%, and C_{FC}=0.13 using BI-2014, ZRB-2002, and I_C cutoff of 2.6.

Earthquake Event(s)	M_W	PGA (g)	Depth to Groundwater (m)	S_T(mm)	S_{V1D} (mm)	$S_{E,L}$ (mm)
Sep-10	7.1	0.18	2.1	21±275	13±20	8±276
Feb-11	6.2	0.40	2.2	151±125	104±50	47±135
Jun-11	6.2	0.26	1.9	79±125	41±25	38±128
Dec-11	6.1	0.30	2.6	-52±175	42±50	-94±182

Notes: S_T = Total settlement (Table 6); S_{V1D} = Average vertical settlement due to volumetric compression using Boulanger and Idriss (2014) (BI-2014), Zhang et al. (2002) (ZRB-2002) procedures and de Greef and Lengkeek (2018) thin-layer correction; $S_{E,L}$ = Ejecta-induced settlement as the difference between the LiDAR-based S_T and S_{V1D}.

Note 3: The uncertainty for volumetric settlement was derived based on the sensitivity of volumetric settlement to PGA, C_{FC}, and P_L for each earthquake event for VsVp 57203 *Shirley Intermediate School* and CC LIQ 1 – CPT 5586 – *Vivian St* sites. Taking the 50th percentile as the baseline case, the minimum and maximum values corresponding to the difference between the 25th percentile and the 50th percentile and the 75th percentile and the 50th percentile were determined. The arithmetic mean of the range of the minimum and maximum difference was evaluated for each patch at the two sites. The maximum arithmetic mean for each earthquake event was rounded to the nearest five and used as the uncertainty value. Accordingly, the 1-D volumetric settlement uncertainties of ±20, ±50, ±25, and ±50 mm for the Sep-10, Feb-11, Jun-11, and Dec-11 earthquake events, respectively, were used for all sites in this study.

Table 9a: Coverage area and height of ejecta estimates for the 10-m buffer using photographs.

Earthquake Event	$A_{E,thick}$ (m^2)	$H_{E,thick}$ (m)	$A_{E,thin}$ (m^2)	$H_{E,thin}$ (m)	A_T (m^2)
Sep-10	0	0	0	0	266
Feb-11	61.4	100-180	46.3	70-150	259*
Jun-11	64.9	50-100	0	0	198*
Dec-11	0	0	0	0	266

Notes: $A_{E,thick/thin}$ =Coverage area of thick/thin ejecta layers; $H_{E,thick/thin}$ = Lower-upper estimate of height of thick/thin ejecta layers; A_T = Total assessment area of a buffer being considered; Thin and thick layers correspond to light gray and dark gray colors of ejecta observed in aerial photographs; * indicates the reduction in the total assessment area due to the shadows in the aerial photograph.

Table 9b: Coverage area and height of ejecta estimates for the 20-m buffer using photographs.

Earthquake Event	$A_{E,thick}$ (m^2)	$H_{E,thick}$ (m)	$A_{E,thin}$ (m^2)	$H_{E,thin}$ (m)	A_T (m^2)
Sep-10	0	0	0	0	729
Feb-11	119	100-180	110	70-150	721*
Jun-11	114	50-100	0	0	598*
Dec-11	0	0	0	0	729

Notes: $A_{E,thick/thin}$ =Coverage area of thick/thin ejecta layers; $H_{E,thick/thin}$ = Lower-upper estimate of height of thick/thin ejecta layers; A_T = Total assessment area of a buffer being considered; Thin and thick layers correspond to light gray and dark gray colors of ejecta observed in aerial photographs; * indicates the reduction in the total assessment area due to the shadows in the aerial photograph.

Table 9c: Coverage area and height of ejecta estimates for the 50-m buffer using photographs.

Earthquake Event	$A_{E,thick}$ (m^2)	$H_{E,thick}$ (m)	$A_{E,thin}$ (m^2)	$H_{E,thin}$ (m)	A_T (m^2)
Sep-10	0	0	0	0	1839
Feb-11	119	100-180	125	70-150	1831*
Jun-11	135	50-100	0	0	1708*
Dec-11	0	0	0	0	1839

Notes: $A_{E,thick/thin}$ =Coverage area of thick/thin ejecta layers; $H_{E,thick/thin}$ = Lower-upper estimate of height of thick/thin ejecta layers; A_T = Total assessment area of a buffer being considered; Thin and thick layers correspond to light gray and dark gray colors of ejecta observed in aerial photographs; * indicates the reduction in the total assessment area due to the shadows in the aerial photograph.

Note 4: The values in Table 9 correspond to the coverage area of ejecta outlined in aerial photographs (Figures 70 through 73) and the lower and upper estimates of ejecta height based on geometry, ground photographs (Figure 74), and EQC LDAT property inspection reports from August 2011 (engineers noted more than 200 mm in height of ejected material in some places under the dwelling in the NW quadrant of the 50-m buffer). The ejecta-induced settlement using the physical evidence and engineering judgment, $S_{E,P}$, is estimated as

$$S_{E,P} = \frac{\sum_{i=1}^{a} A_{E,thick,i} * H_{E,thick,i} + \sum_{j=1}^{b} A_{E,thin,j} * H_{E,thin,j}}{A_T} = \frac{\sum_{i=1}^{a} V_{E,thick,i} + \sum_{j=1}^{b} V_{E,thin,j}}{A_T}$$

where

- $A_{E,thick,i}$ and $H_{E,thick,i}$ are the area and the height of a thick ejecta layer, respectively;
- $A_{E,thin,j}$ and $H_{E,thin,j}$ are the area and the height of a thin ejecta layer, respectively;
- A_T is the total assessment area for a buffer being considered (Figure 1).

Table 10: Ejecta-induced settlement estimates for Patch A based on photographs.

Earthquake Event	10-m buffer		20-m buffer		50-m buffer	
	$S_{E,P,lower}$ (mm)	$S_{E,P,upper}$ (mm)	$S_{E,P,lower}$ (mm)	$S_{E,P,upper}$ (mm)	$S_{E,P,lower}$ (mm)	$S_{E,P,upper}$ (mm)
Sep-10	0	0	0	0	0	0
Feb-11	36	70	27	53	11	22
Jun-11	16	33	10	19	4	8
Dec-11	0	0	0	0	0	0

Note: $S_{E,P,lower}$ and $S_{E,P,upper}$ correspond to lower and upper estimates of $S_{E,P}$, respectively.

Table 11: Best final estimates of ejecta-induced settlement for Patch A.

EQ Event	10-m buffer			20-m buffer			50-m buffer		
	$S_{E,L}$ (mm)	$S_{E,P}$ (mm)	$S_{E,final}$ (mm)	$S_{E,L}$ (mm)	$S_{E,P}$ (mm)	$S_{E,final}$ (mm)	$S_{E,L}$ (mm)	$S_{E,P}$ (mm)	$S_{E,final}$ (mm)
Sep-10	12 ± 276	0	0	2 ± 276	0	0	8 ± 276	0	0
Feb-11	68 ± 135	53 ± 17	60 ± 45	49 ± 135	40 ± 13	45 ± 45	47 ± 135	17 ± 5	30 ± 45
Jun-11	44 ± 128	25 ± 8	35 ± 65	34 ± 128	12 ± 4	25 ± 65	38 ± 128	6 ± 2	20 ± 65
Dec-11	-63 ± 182	0	0	-79 ± 182	0	0	-94 ± 182	0	0

Notes: $S_{E,L}$ = Ejecta-induced settlement based on LiDAR data reported in Table 8; $S_{E,P}$ = Median ejecta-induced settlement for the range of values reported in Table 10; $S_{E,final}$ = Best final estimate of ejecta-induced settlement rounded to the nearest 5; Final plus/minus values are also rounded to the nearest 5.

Note 5:

- $S_{E,final}$ for the Sep-10 and Dec-11 EQs is based solely on $S_{E,P}$ because the photographic evidence does not indicate the presence of ejecta following the two events. The aerial photograph for the Dec-11 EQ shows no fresh ejecta at the site and no ejecta in the neighborhood (only negligible quantum on the road), and shows the cleaning traces of ejecta from the previous earthquake(s).
- $S_{E,final}$ for the Feb-11 is the weighted average of $S_{E,L}$ and $S_{E,P}$ with the weight coefficients of 1/3 and 2/3, respectively.
- The aerial photograph for the Jun-11 EQ indicates fresh ejecta at the site and significant quantum of ejected material in the neighborhood (especially on the road). The weight coefficients used to calculate $S_{E,final}$ for the Jun-11 EQ are 1/2 for both $S_{E,L}$ and $S_{E,P}$.
- The uncertainty associated with $S_{E,final}$ is also the weighted average of uncertainties associated with $S_{E,L}$ and $S_{E,P}$ and their corresponding weights.
- The weights are based on the LiDAR error bands, LPI prediction error (Maurer et al. 2014[3]), presence of ejecta at the time of LiDAR surveys, and completeness of visual evidence (i.e., ground and aerial photographs and EQC LDAT property inspection reports for the site). The Avondale Playground site is not in the apparent zone of higher/lower ground surface subsidence for the Sep-10, Feb-11, or Jun-11 EQs (i.e., the overestimate/underestimate of the ground surface elevation by LiDAR surveys). The site is in the zone of accurate LPI prediction

[3] Maurer, B. W., Green, R. A., Cubrinovski, M., & Bradley, B. A. (2014). Evaluation of the Liquefaction Potential Index for Assessing Liquefaction Hazard in Christchurch, New Zealand. *Journal of Geotechnical and Geoenvironmental Engineering*, 140(7), 04014032-1-11. doi:10.1061/(asce)gt.1943-5606.0001117

of liquefaction severity for the Sep-10 EQ and slight LPI underprediction of liquefaction severity for the Feb-11 EQ. The ejecta appear to be present at the site during all post Feb-11 LiDAR surveys (except for the Oct-15 LiDAR survey, which was excluded from the analysis due to the anthropogenic changes). The LDAT property inspection report is available for nearby properties. There are no ground photographs of the assessment area only for a property within the 50-m buffer.

<u>Summary 1</u>:

The best estimate of the ejecta-induced free-field ground settlement at the Avondale Playground site for the SEP 2010, FEB 2011, JUN 2011, and DEC 2011 earthquake is 0 mm, 60±45 mm, 35±65 mm (mean = 35 mm, range = 0-100 mm), and 0 mm, respectively.

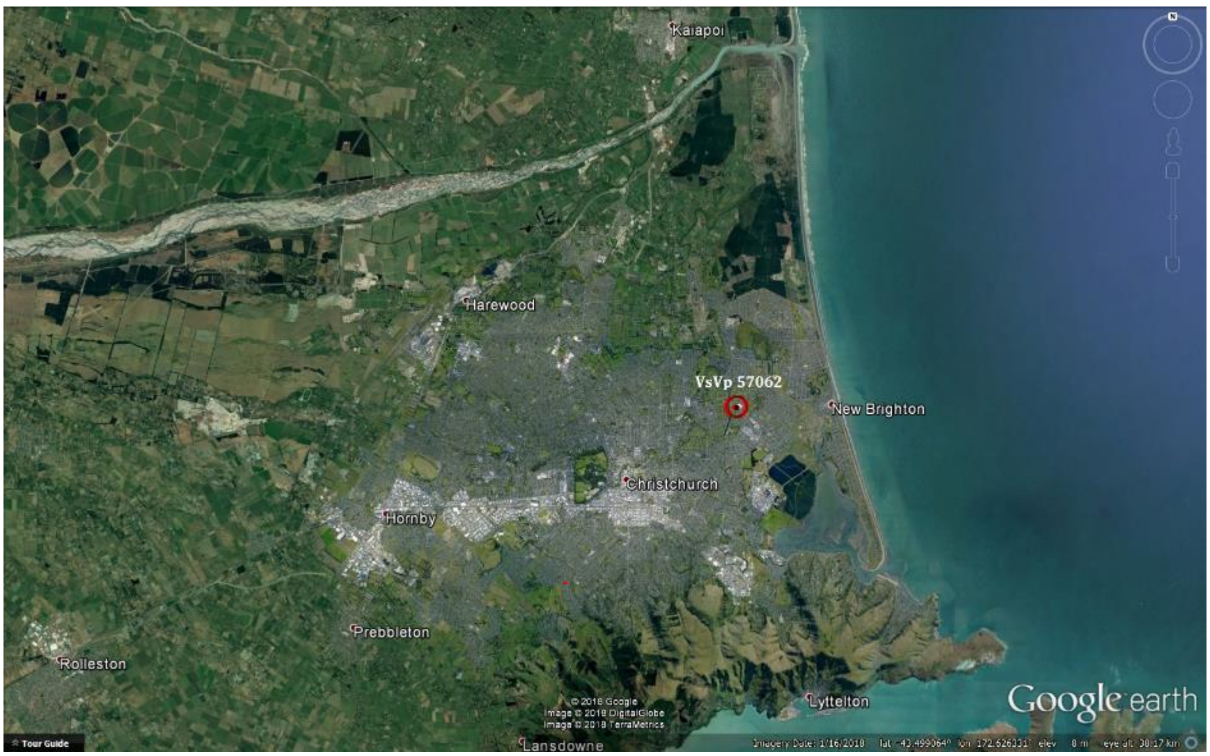

Figure 5: Location of the site.

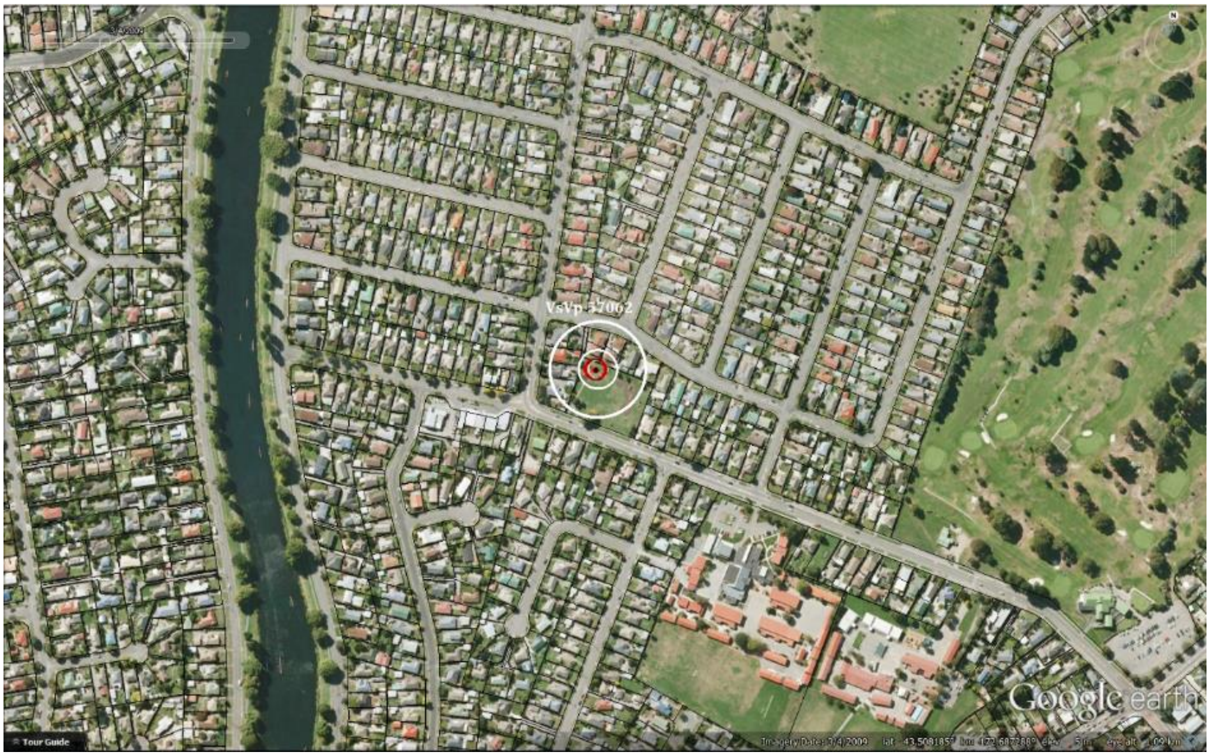

Figure 6: Position of the site relative to nearby buildings, vegetation, and free-face features.

Figure 7: Sreet view of the flat land.

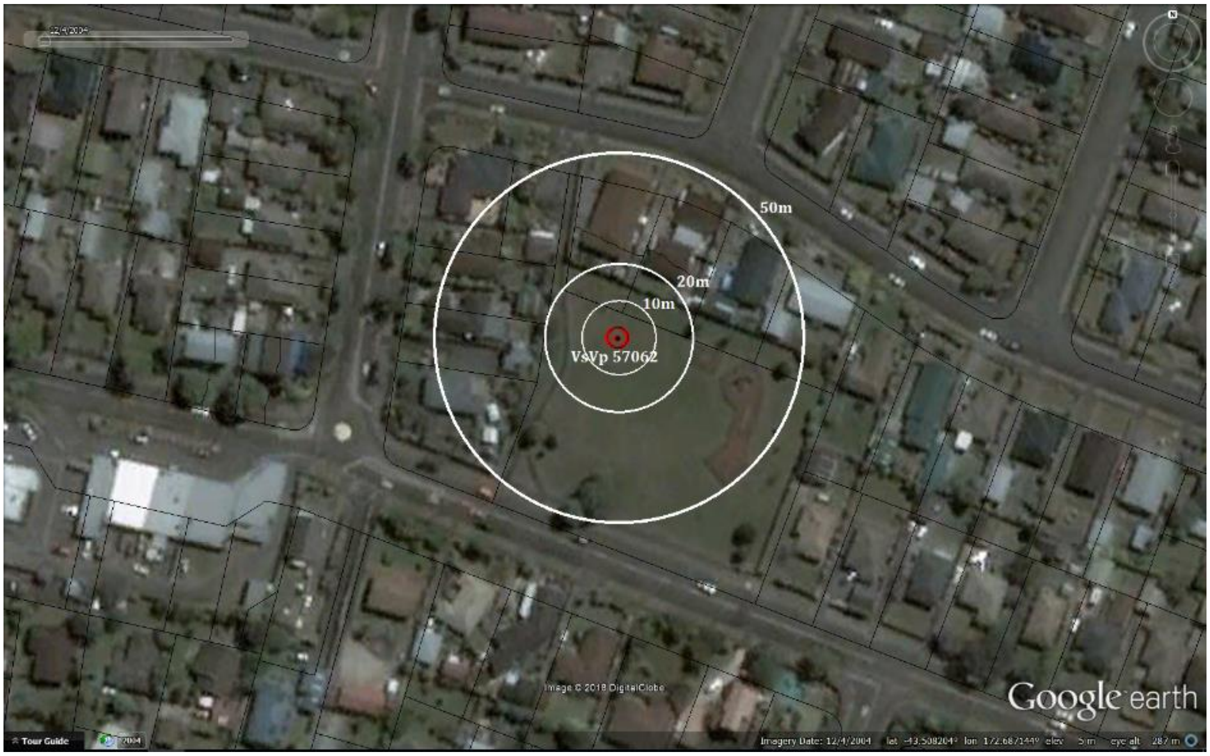

Figure 8: Satellite image of the site taken in Dec 2004.

Figure 9: Satellite image of the site taken on Sep 04, 2010.

Figure 10: Satellite image of the site taken on Feb 27, 2011.

Figure 11: Satellite image of the site taken in Apr 2012.

Figure 12: Satellite image of the site taken in Jan 2013.

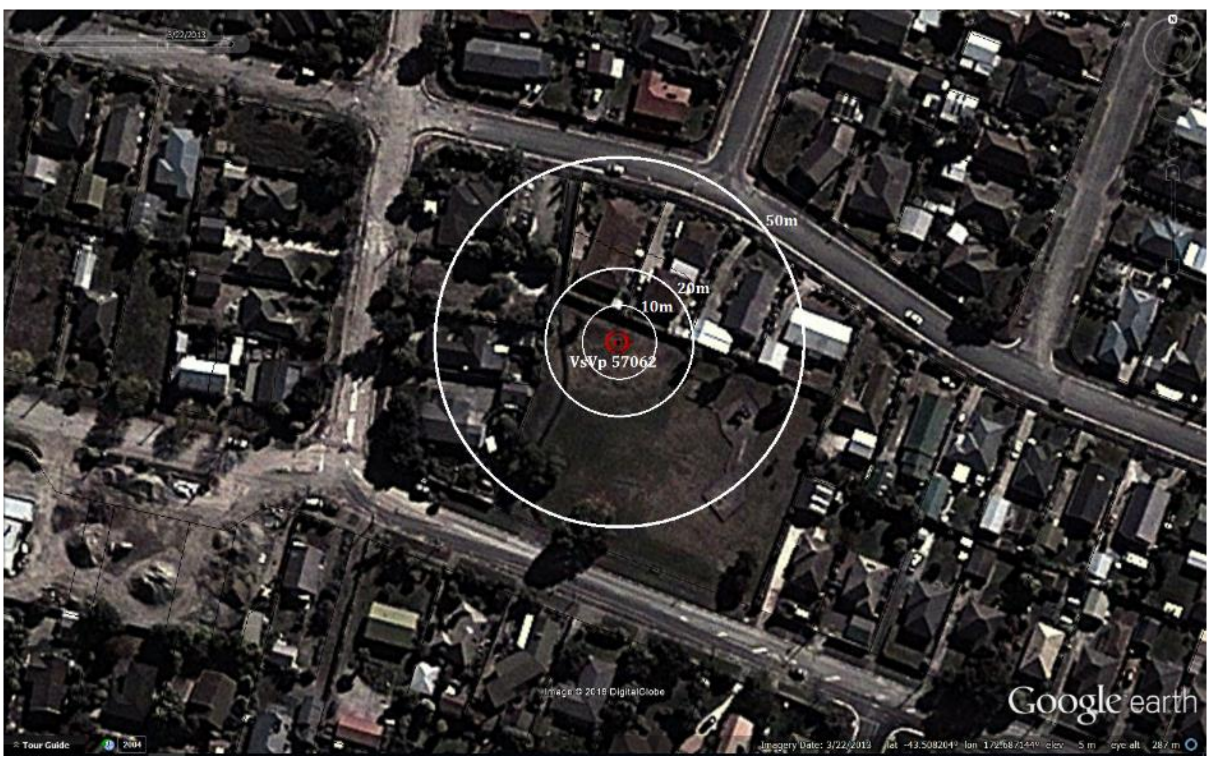

Figure 13: Satellite image of the site taken in March 2013.

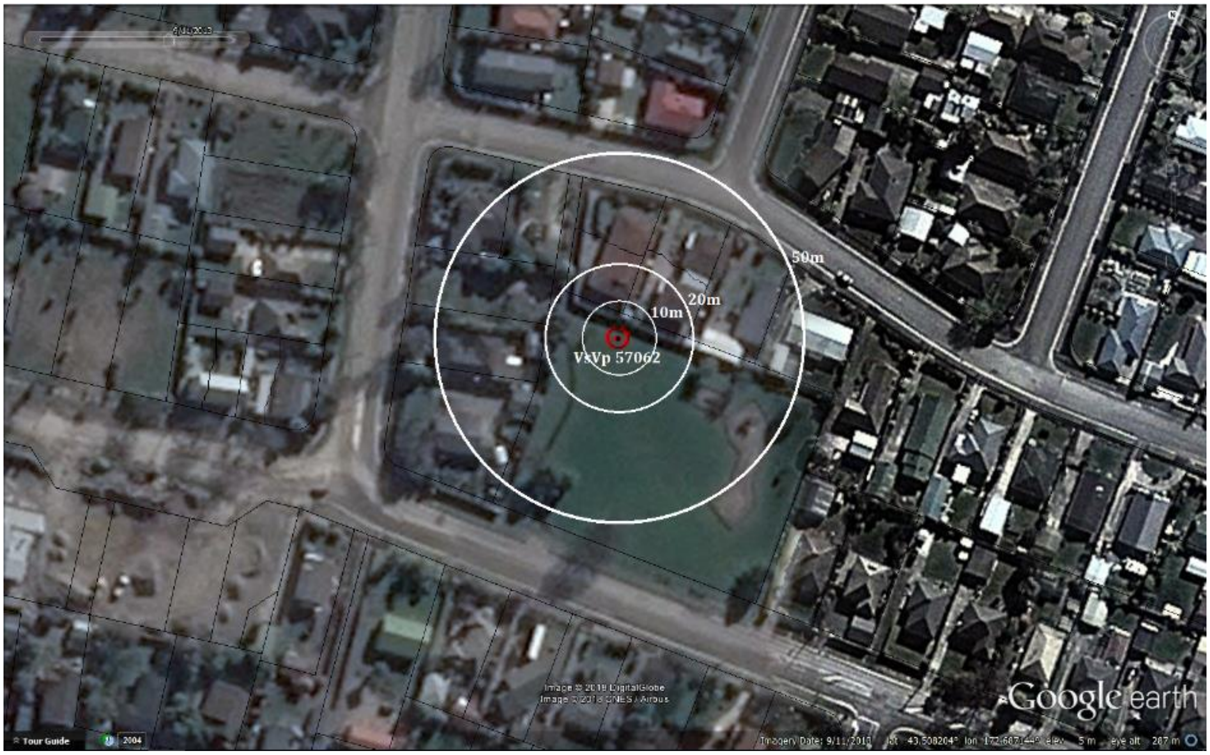

Figure 14: Satellite image of the site taken in Sep 2013.

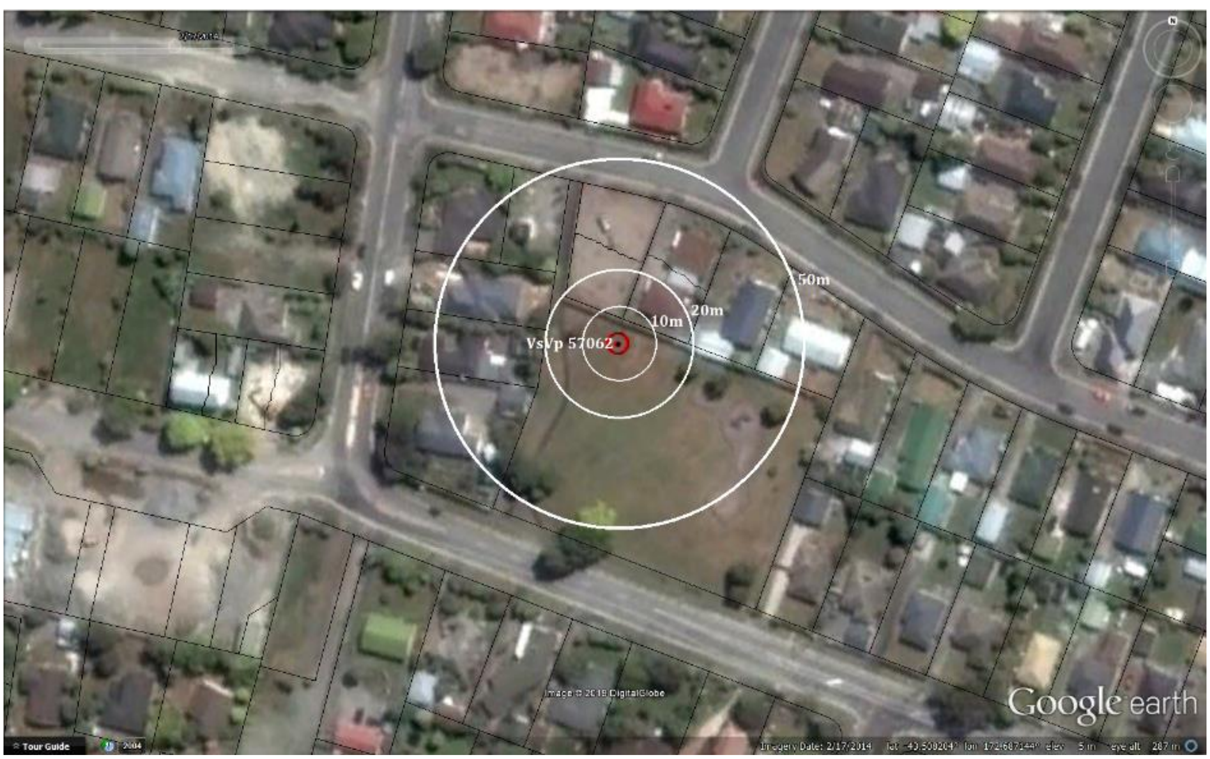

Figure 15: Satellite image of the site taken in Feb 2014.

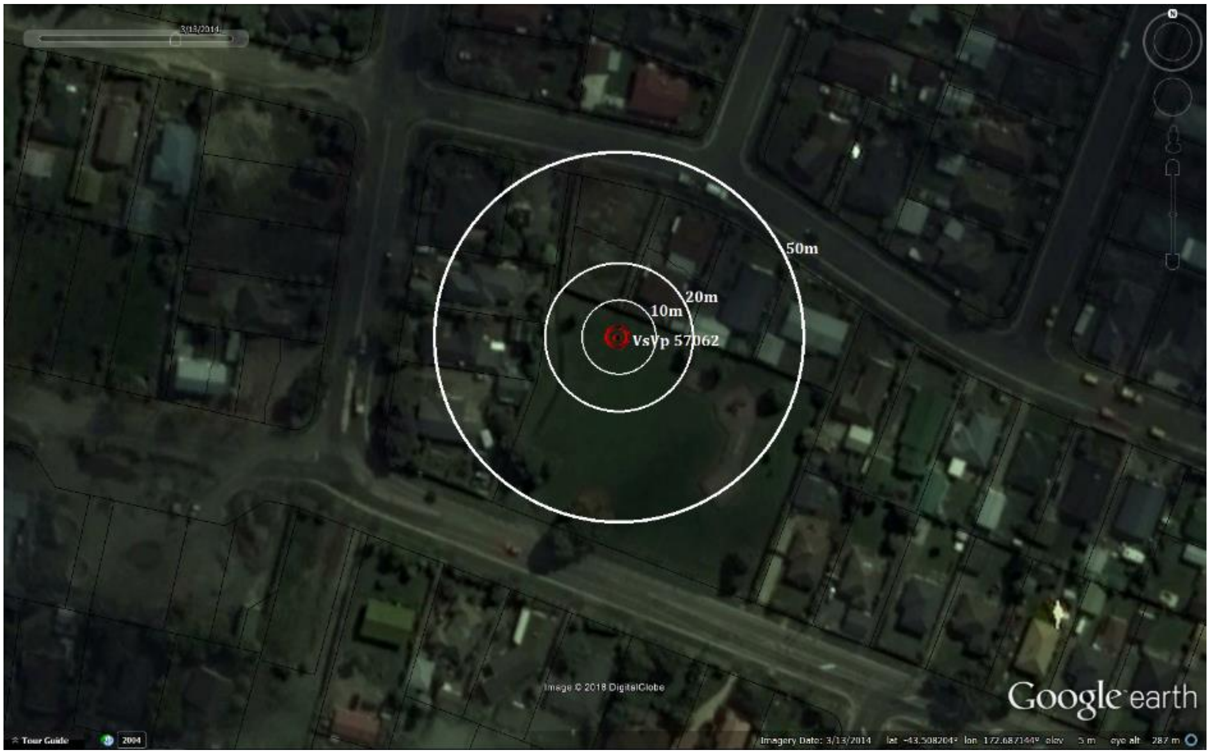

Figure 16: Satellite image of the site taken in March 2014.

Figure 17: Satellite image of the site taken in Aug 2014.

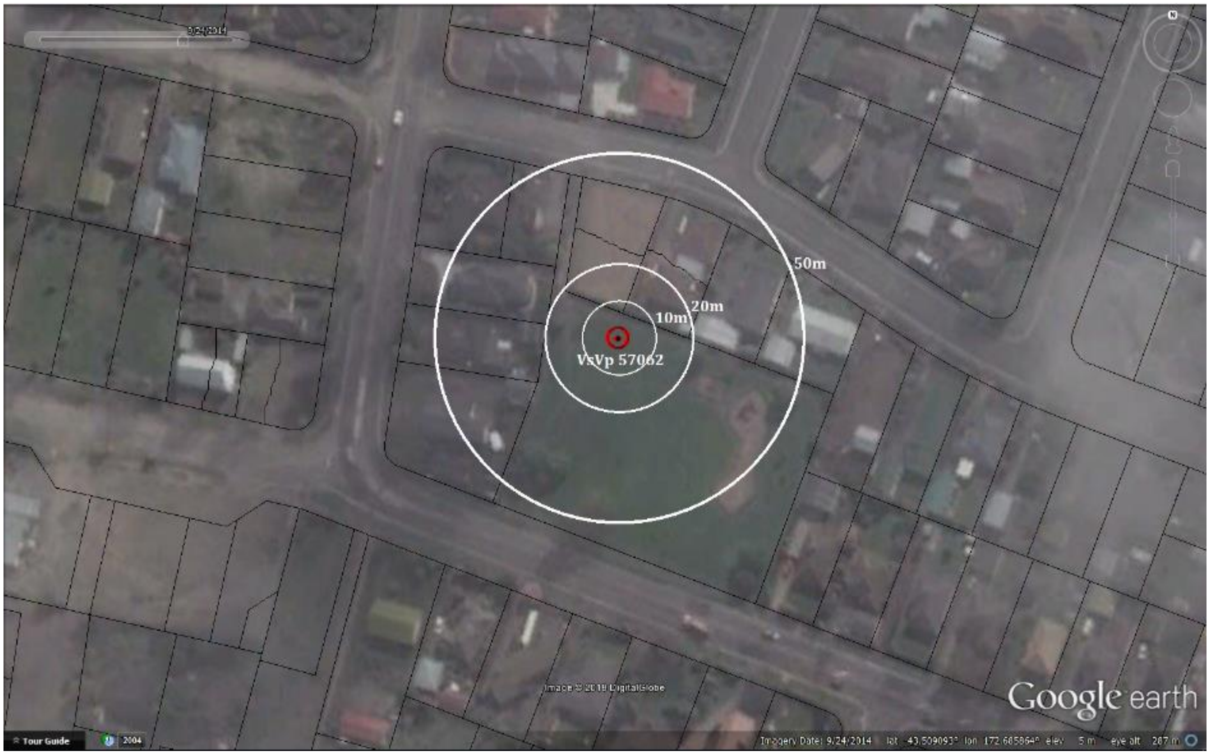

Figure 18: Satellite image of the site taken in Sep 2014.

Figure 19: Satellite image of the site taken in Apr 2015.

Figure 20: Satellite image of the site taken in July 2015.

Figure 21: Satellite image of the site taken in Feb 2016.

Figure 22: EQC Aerial Photograph of the site taken Sep 4, 2010.

Figure 23: EQC Aerial Photograph of the site taken on Feb 24, 2011.

Figure 24: EQC Aerial Photograph of the site taken on June 14-15, 2011.

Figure 25: EQC Aerial Photograph of the site taken on June 16, 2011.

Figure 26: EQC Aerial Photograph of the site taken on Dec 24, 2011.

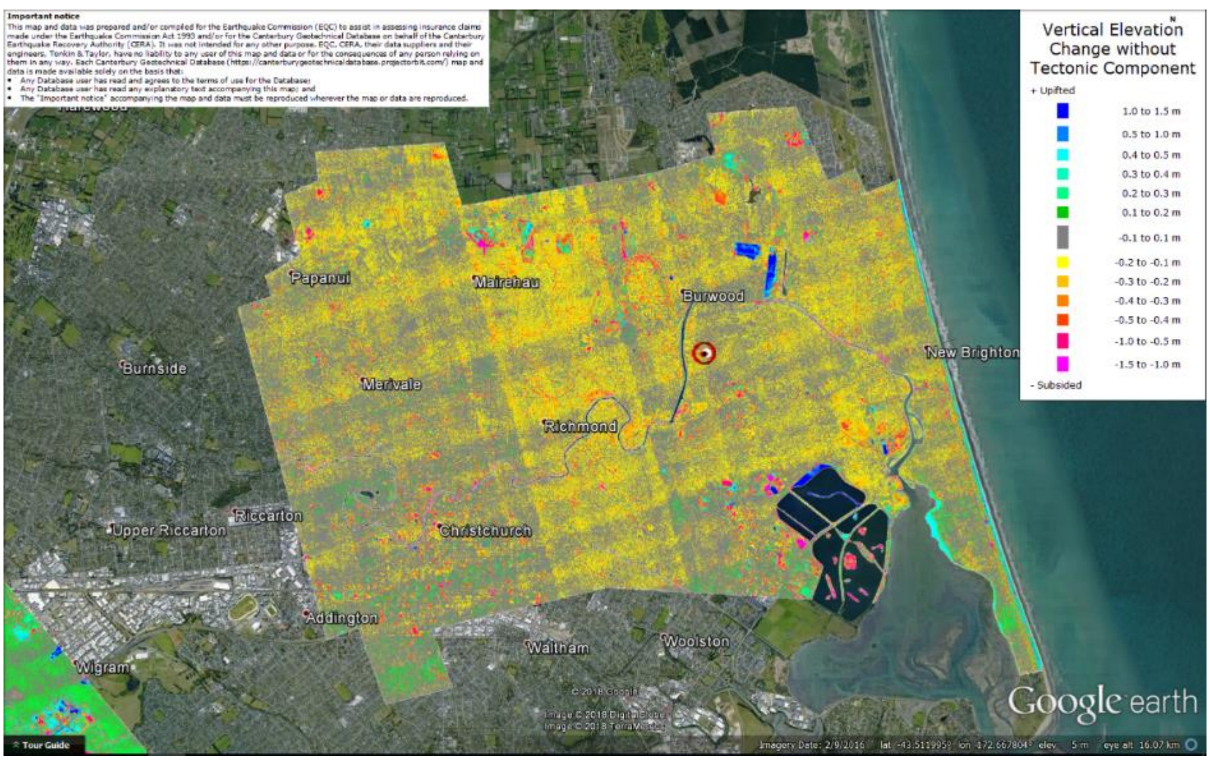

Figure 27: Vertical Ground Movements (Surface – Tectonic) for Sep 2010 Earthquake – the site is not in the apparent zone of overestimated ground surface subsidence.

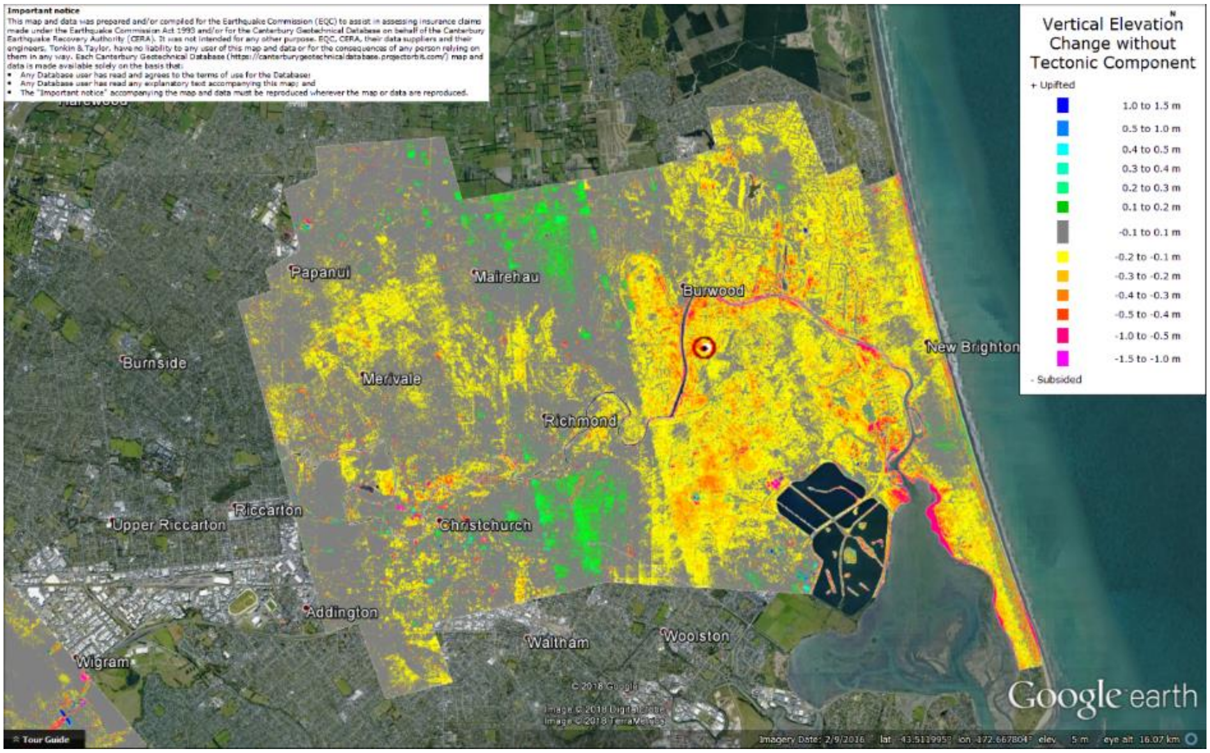

Figure 28: Vertical Ground Movements (Surface – Tectonic) for Feb 2011 Earthquake – the site is not in the apparent zone of underestimated ground surface subsidence.

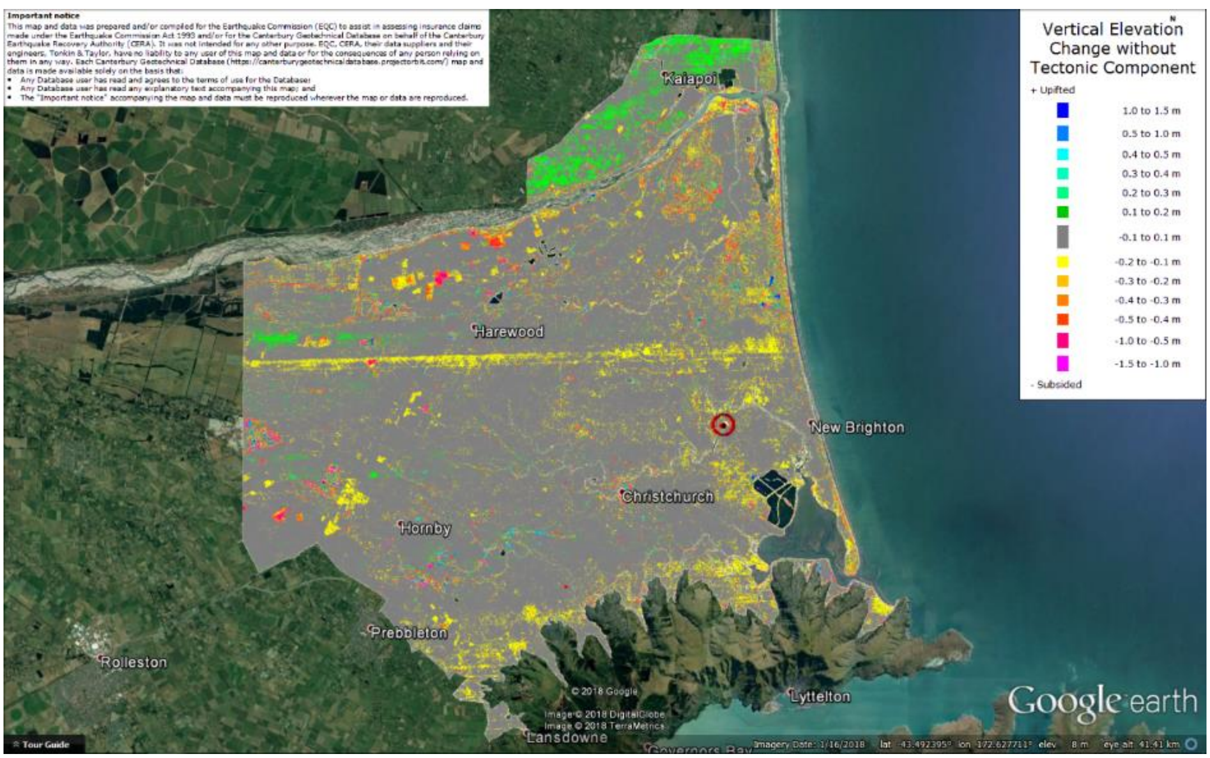

Figure 29: Vertical Ground Movements (Surface – Tectonic) for June 2011 Earthquake – the site is not in the apparent zone of overestimated or underestimated ground surface subsidence.

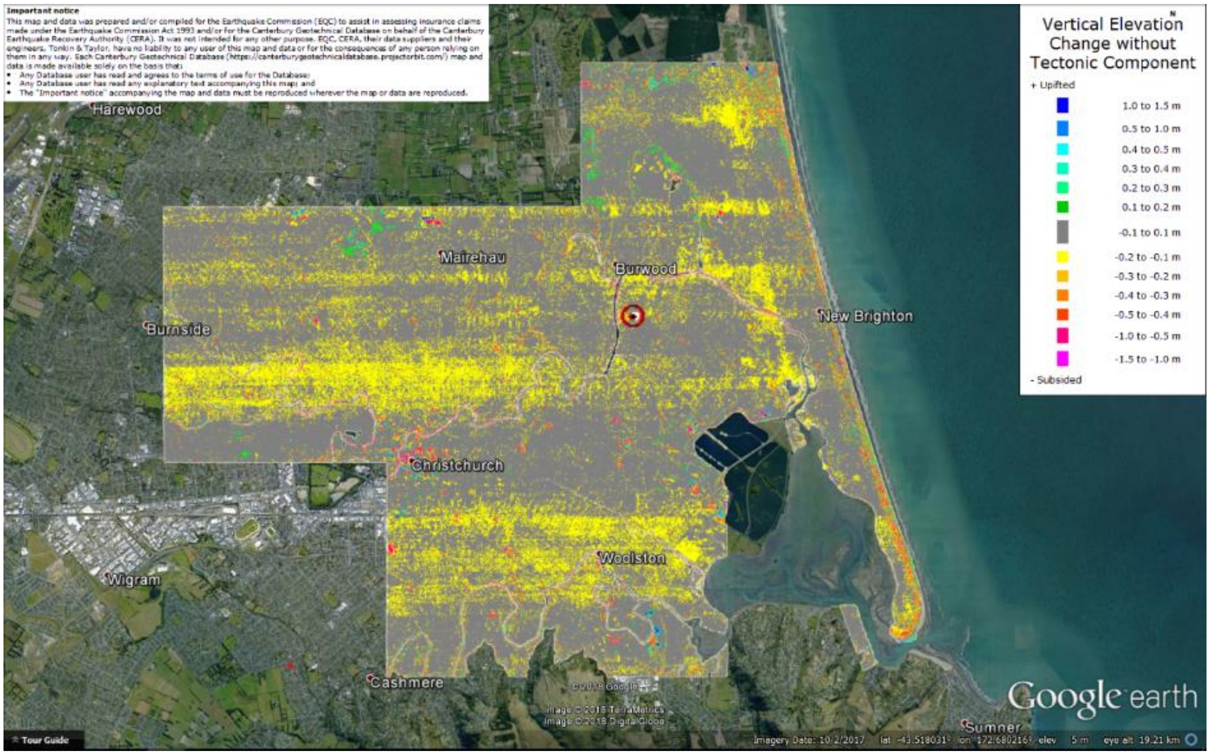

Figure 30: Vertical Ground Movements (Surface – Tectonic) for Dec 2011 Earthquake – the site is not in the apparent zone of overestimated or underestimated ground surface subsidence.

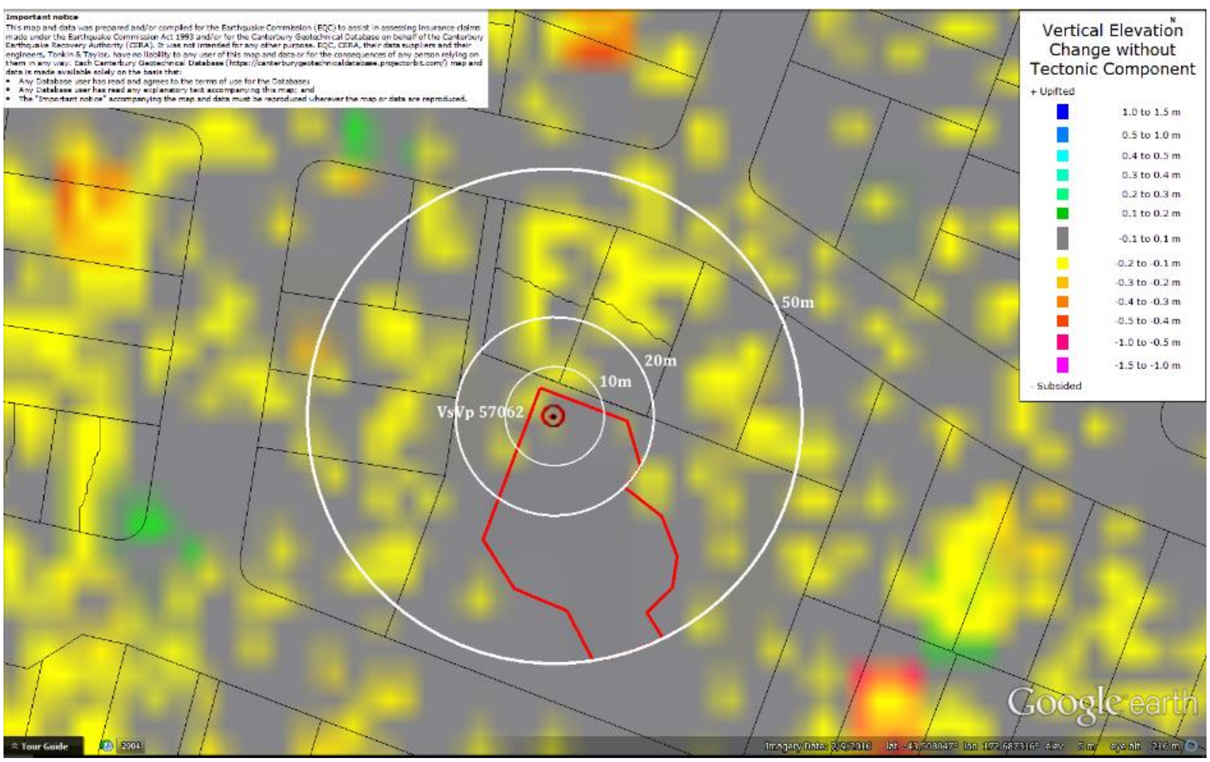

Figure 31: Ground surface subsidence without tectonic component for Sep 2010 Earthquake according to the LiDAR DEM.

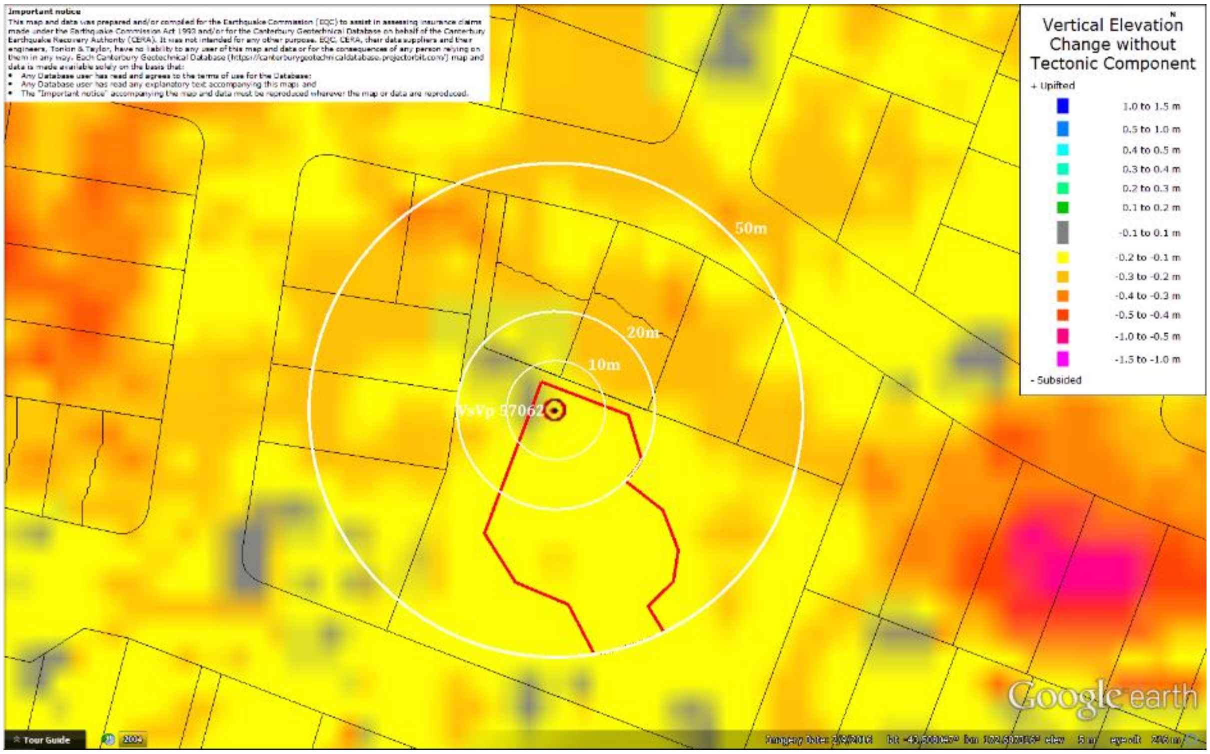

Figure 32: Ground surface subsidence without tectonic component for Feb 2011 Earthquake according to the LiDAR DEM.

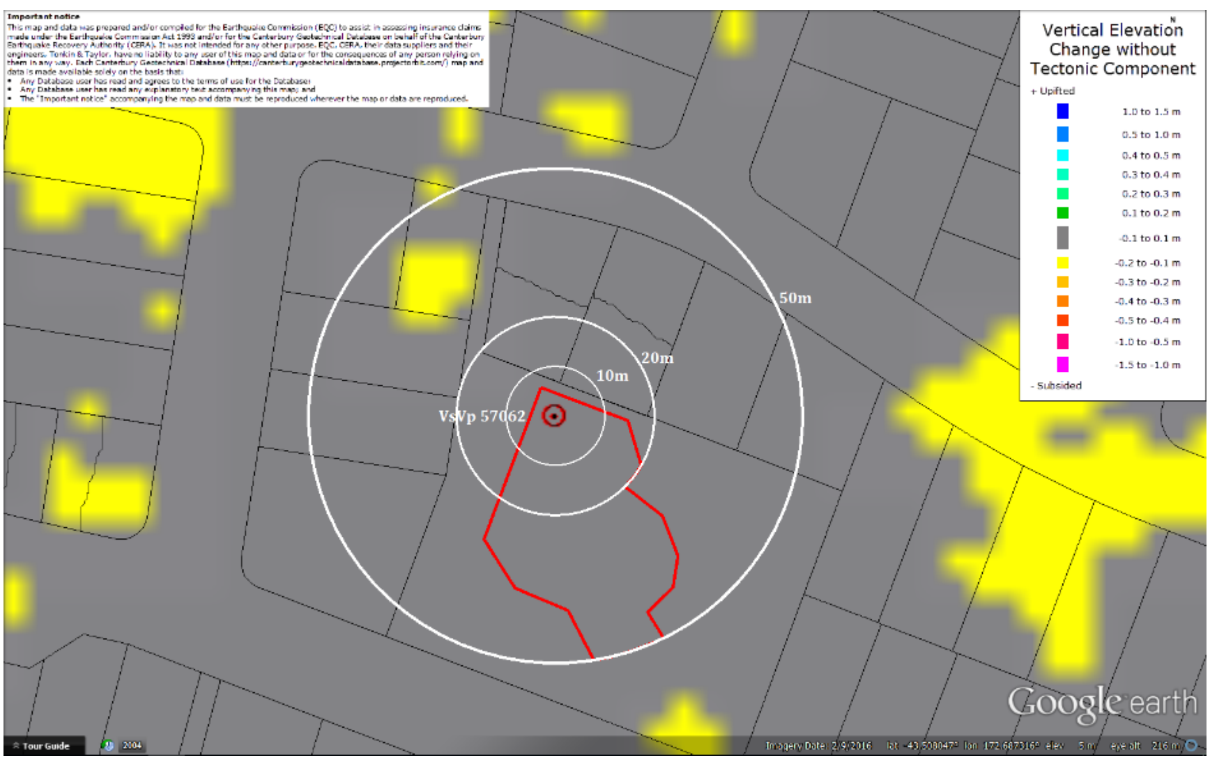

Figure 33: Ground surface subsidence without tectonic component for June 2011 Earthquake according to the LiDAR DEM.

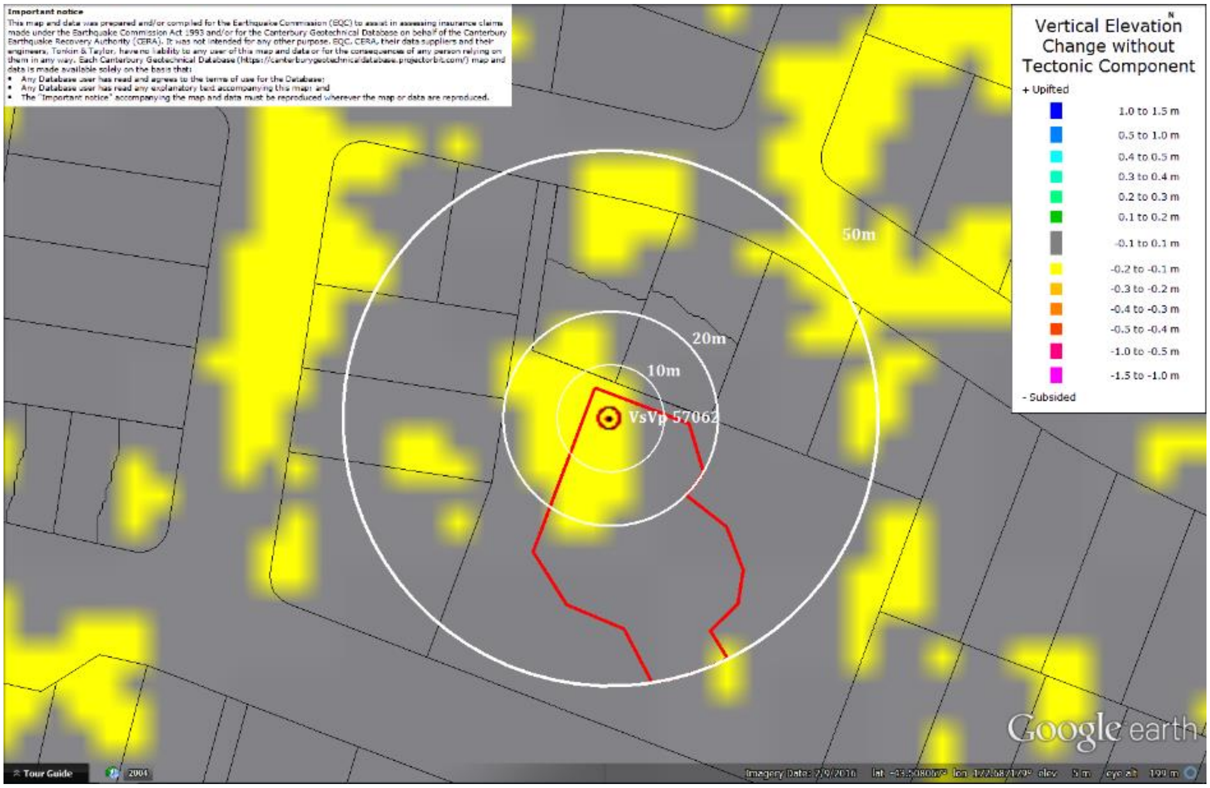

Figure 34: Ground surface subsidence without tectonic component for Dec 2011 Earthquake according to the LiDAR DEM.

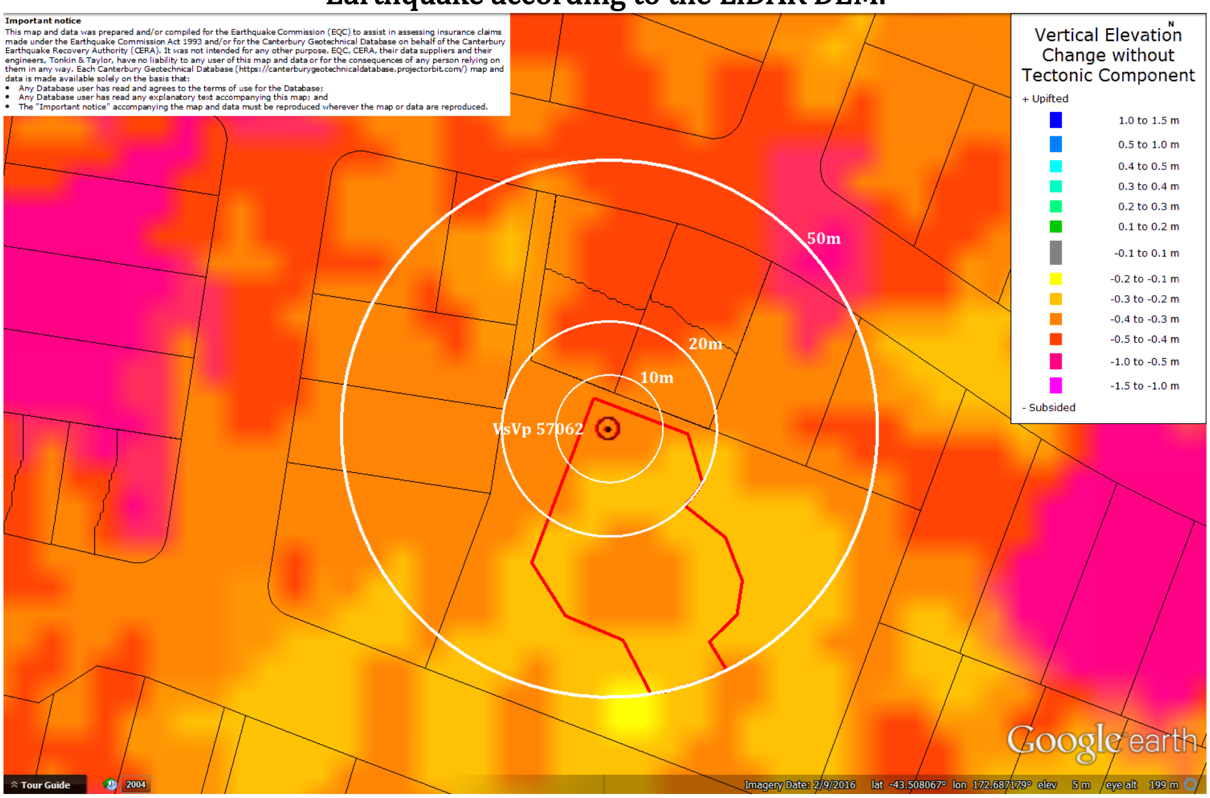

Figure 35: Ground surface subsidence without tectonic component for Canterbury Earthquake Sequence according to the LiDAR DEM.

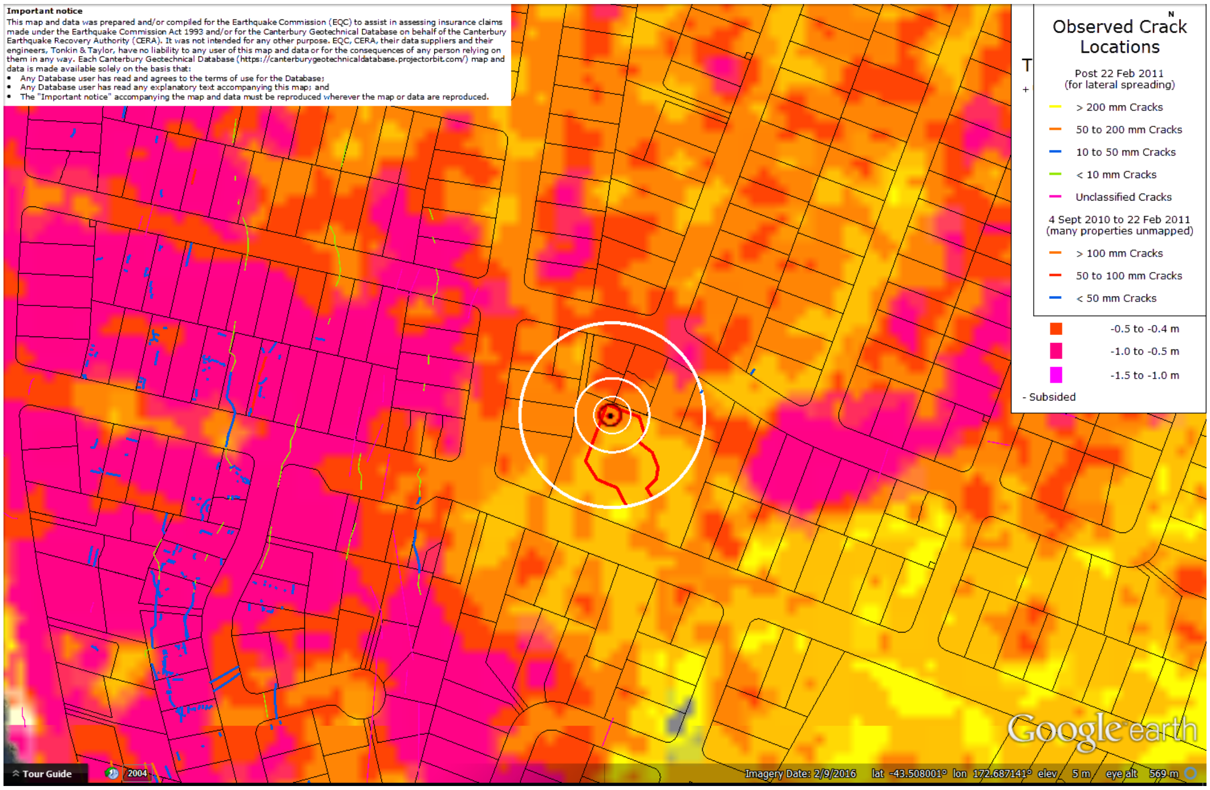

Figure 36: Absence of significant ground cracks indicating no lateral spreading for Canterbury Earthquake Sequence.

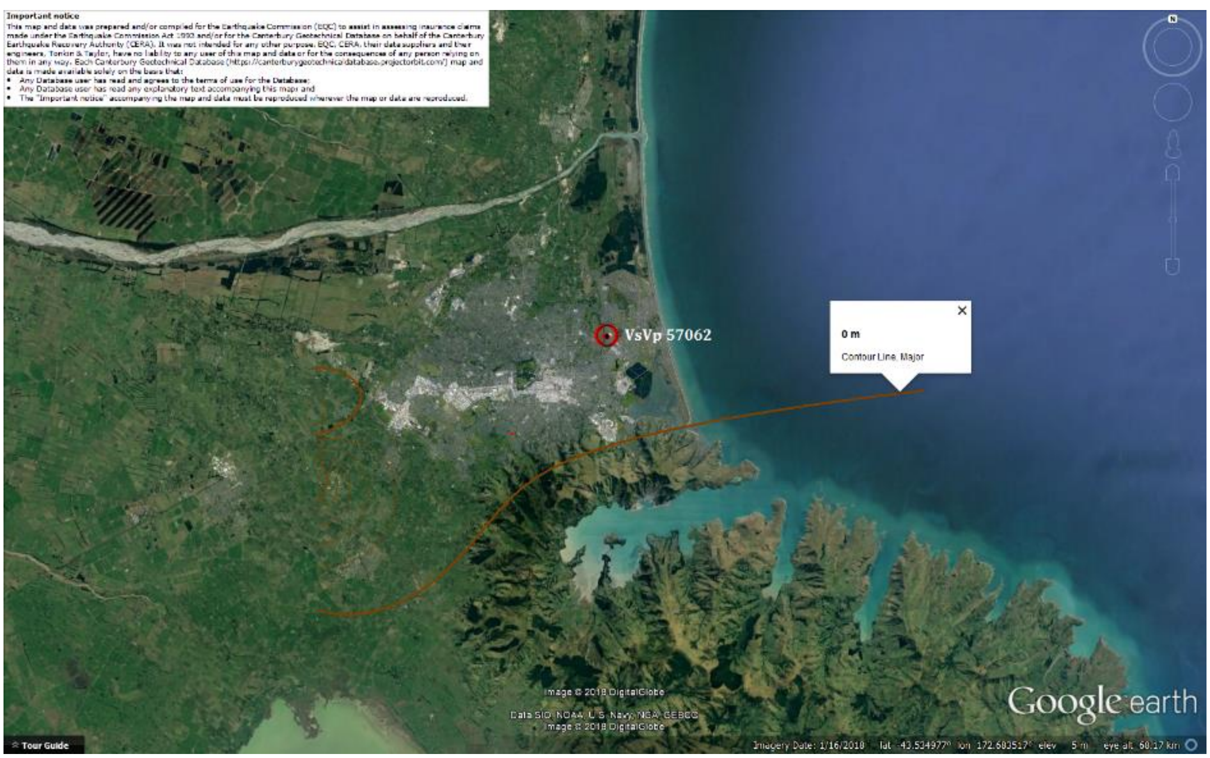

Figure 37: Vertical tectonic movements for Sep 2010 Earthquake.

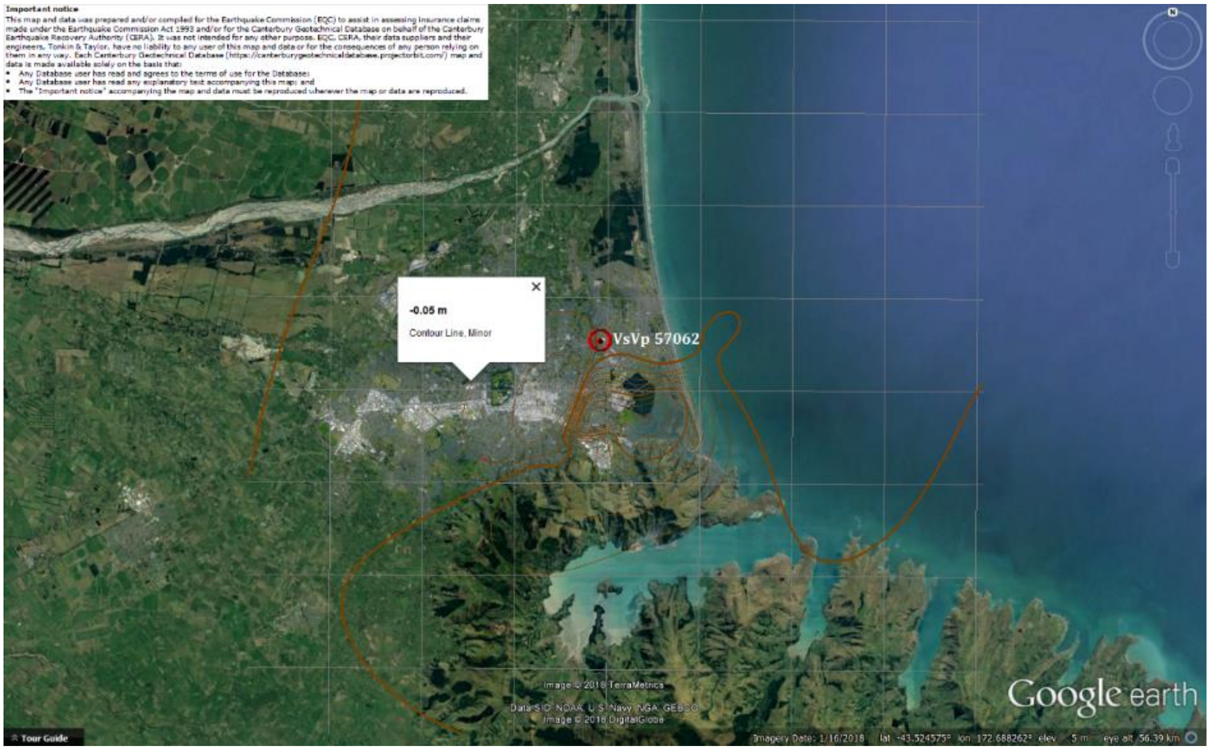

Figure 38: Vertical tectonic movements for Feb 2011 Earthquake.

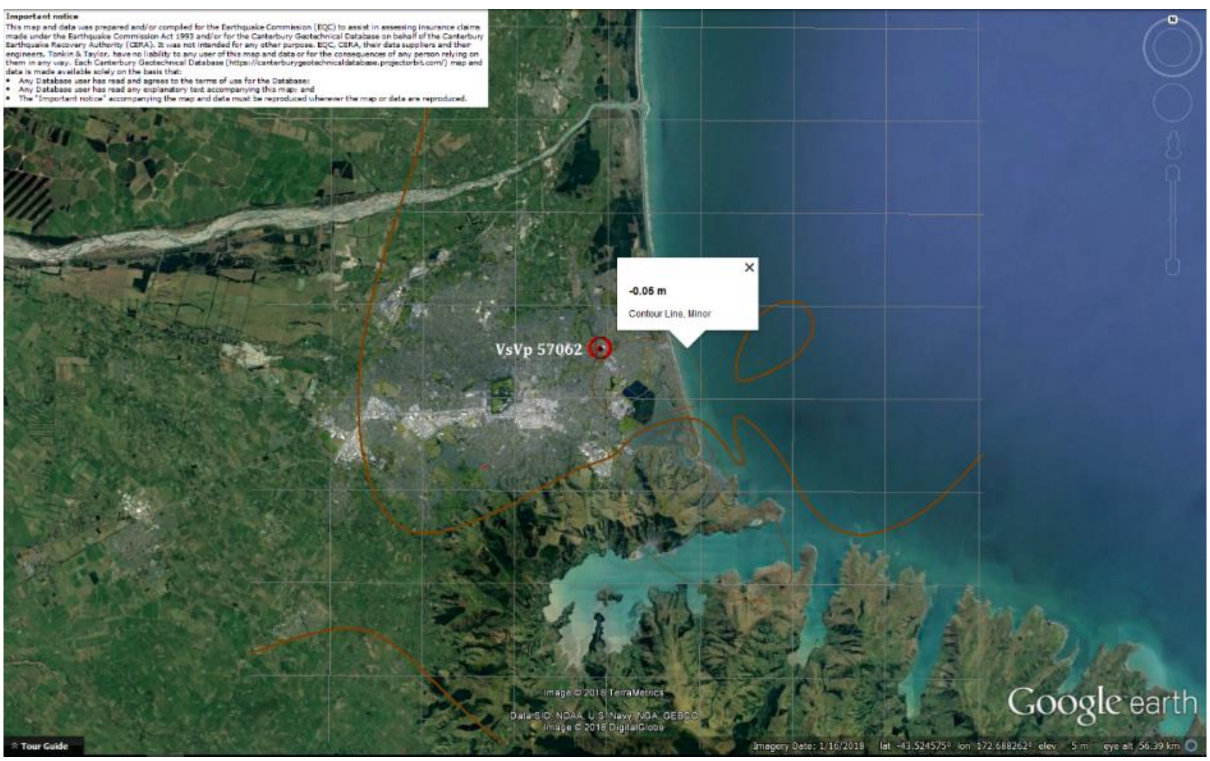

Figure 39: Vertical tectonic movements for June 2011 Earthquake.

Figure 40: Vertical tectonic movements for Dec 2011 Earthquake.

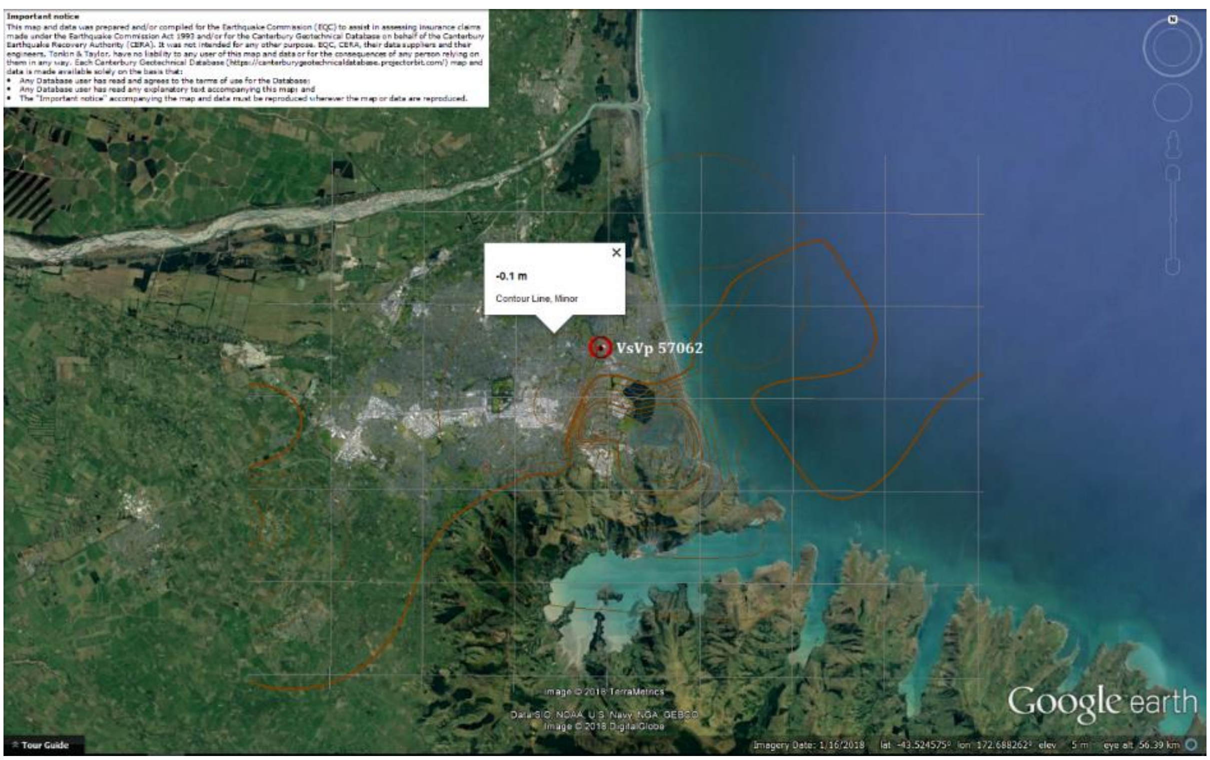

Figure 41: Vertical tectonic movements for Canterbury Earthquake Sequence.

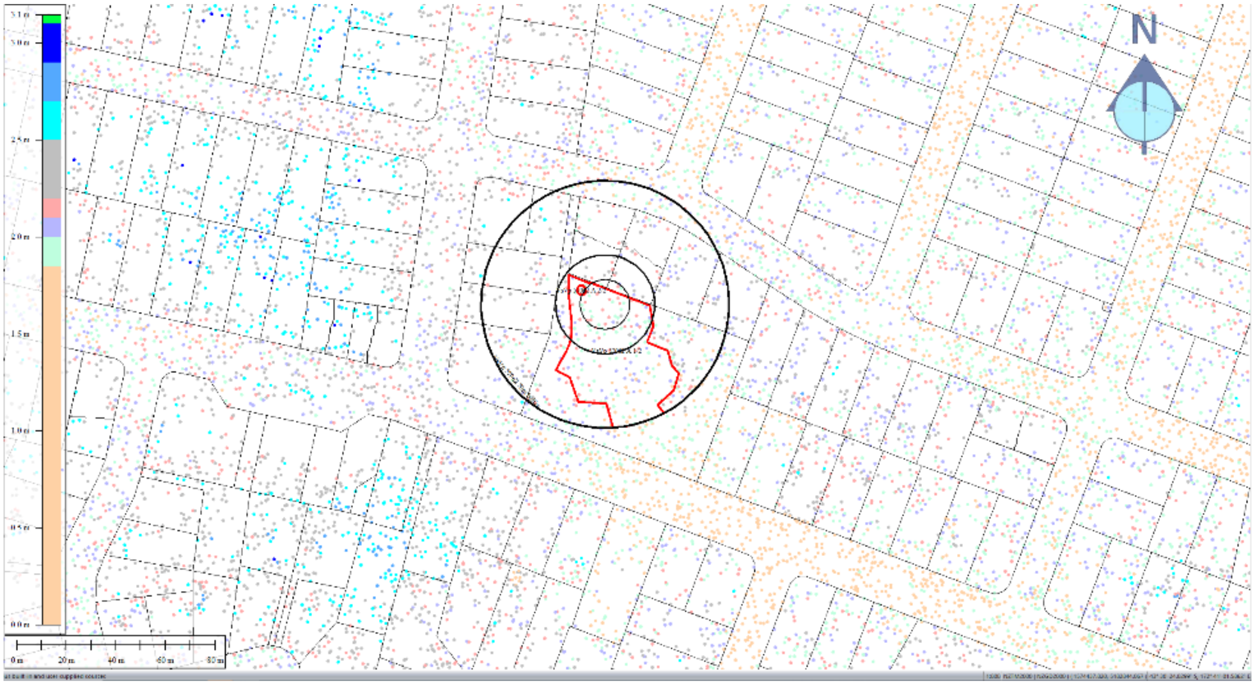

Figure 42: Jul 2003 LiDAR survey.

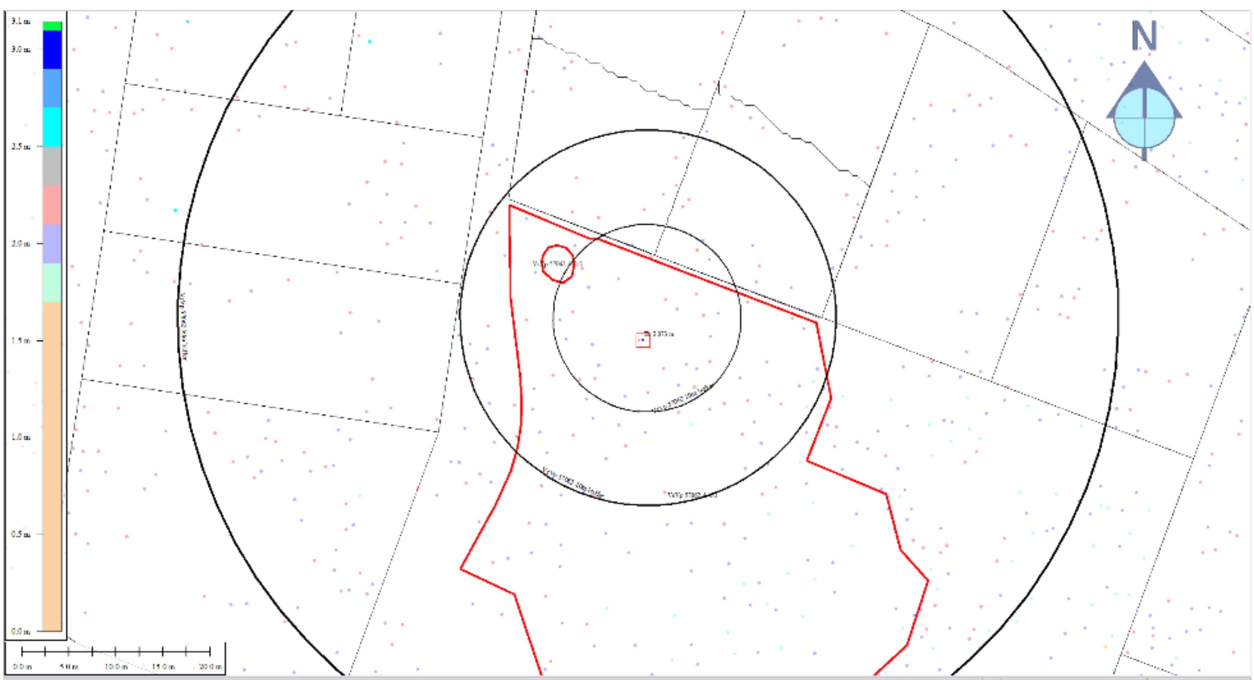

Figure 43: Ground surface elevation averaged over 10-m buffer for Jul 2003 LiDAR survey.

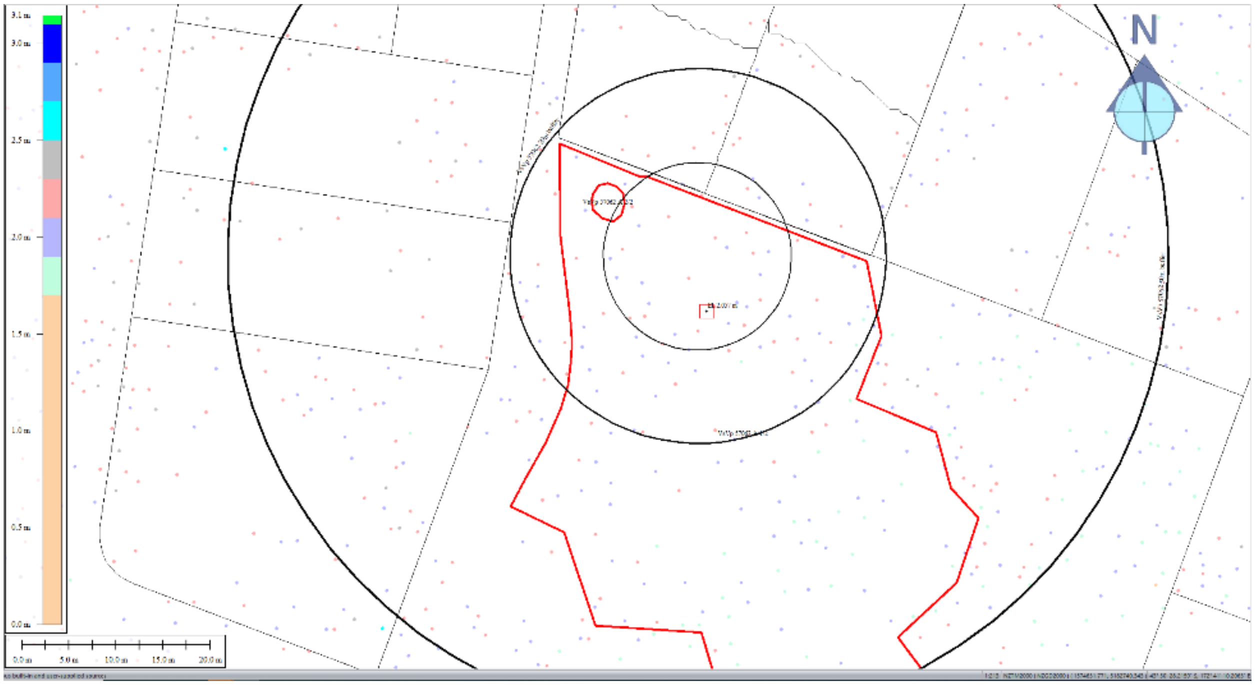

Figure 44: Ground surface elevation averaged over 20-m buffer for Jul 2003 LiDAR survey.

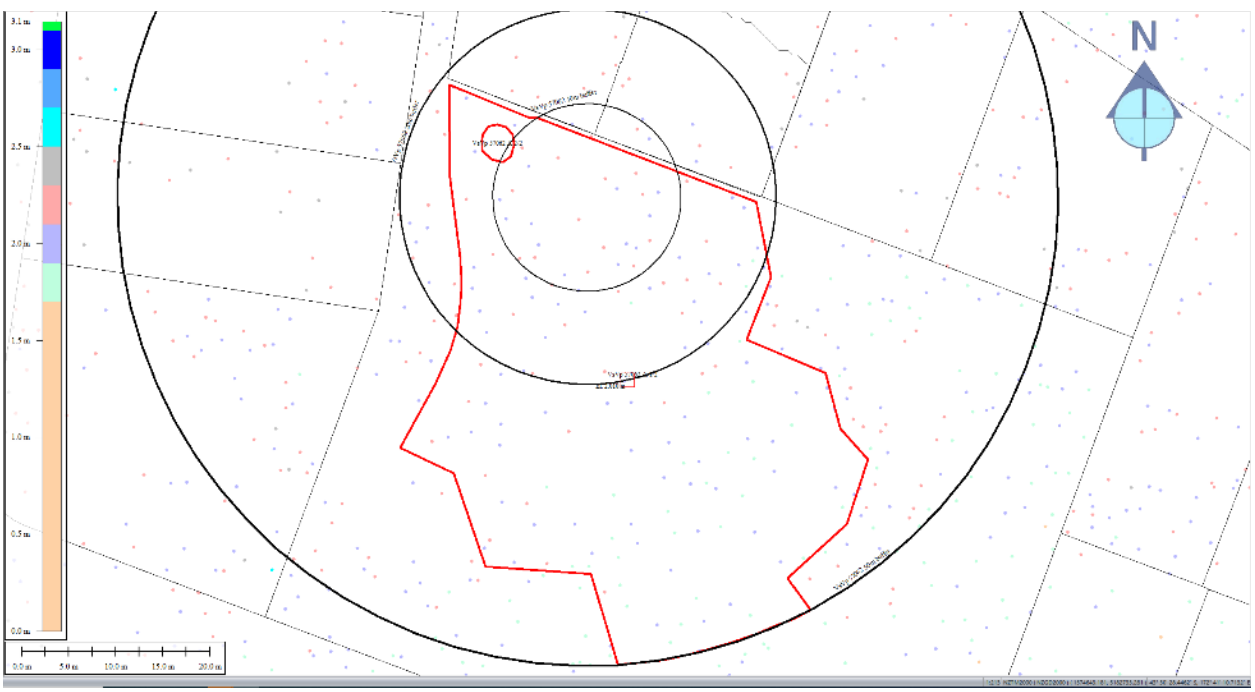

Figure 45: Ground surface elevation averaged over 50-m buffer for Jul 2003 LiDAR survey.

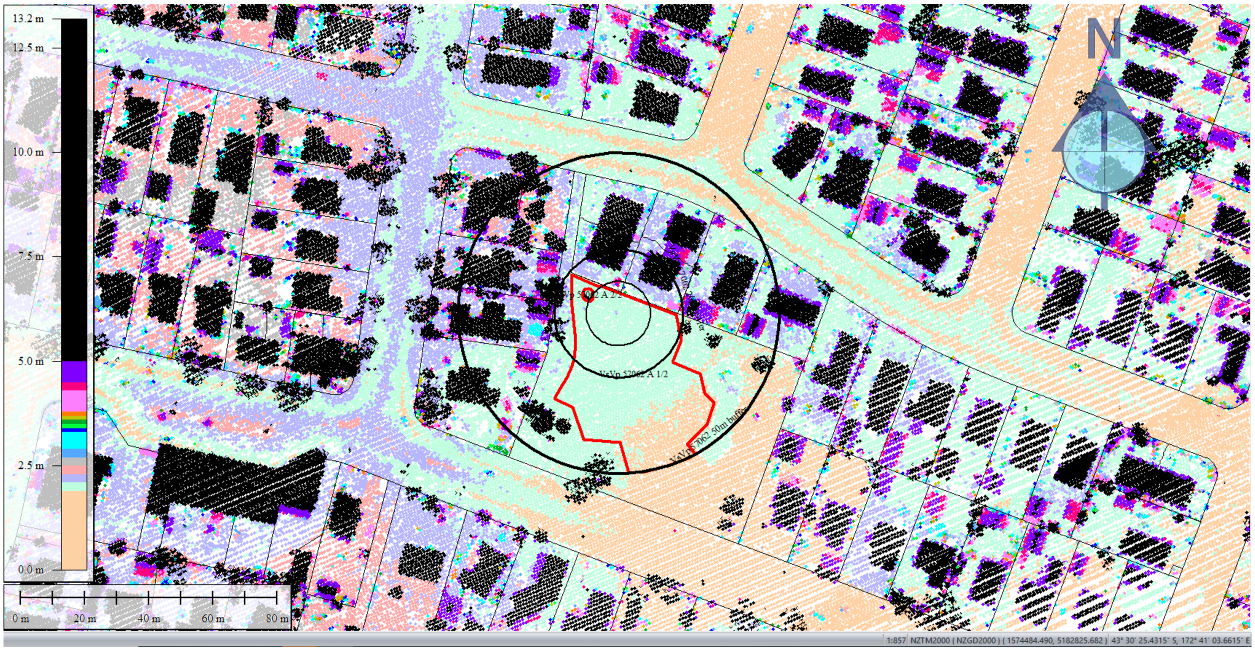

Figure 46: Sep 5, 2010 LiDAR survey.

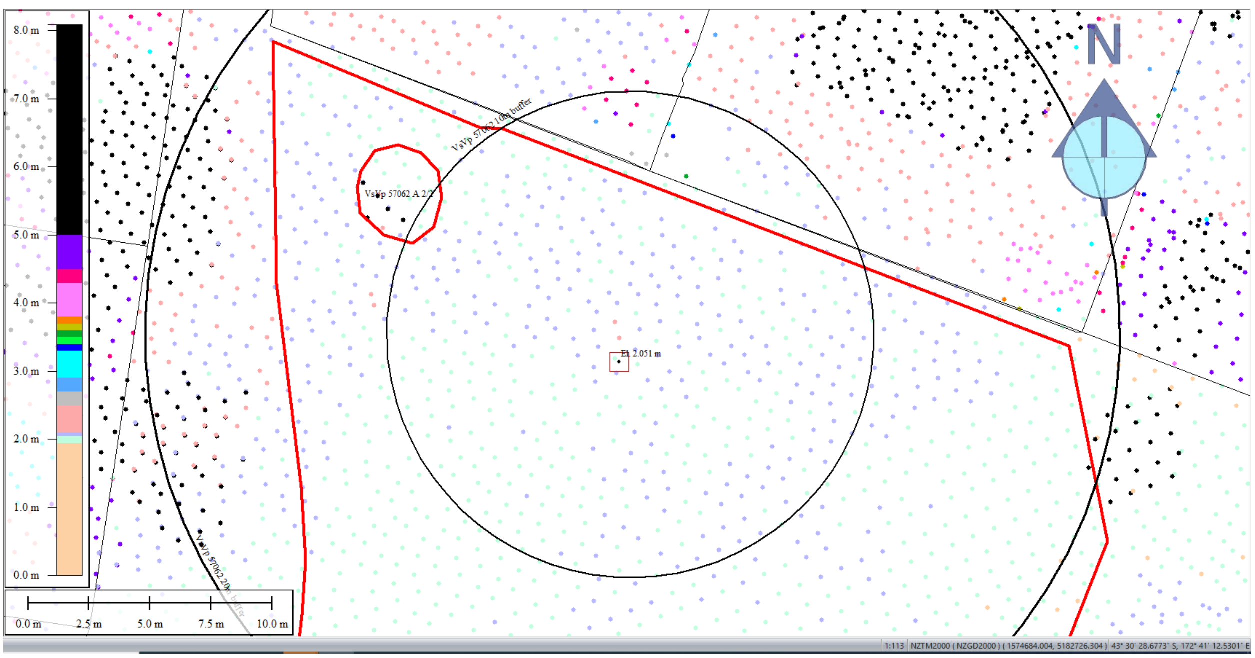

Figure 47: Ground surface elevation averaged over 10-m buffer for Sep 5, 2010 LiDAR survey.

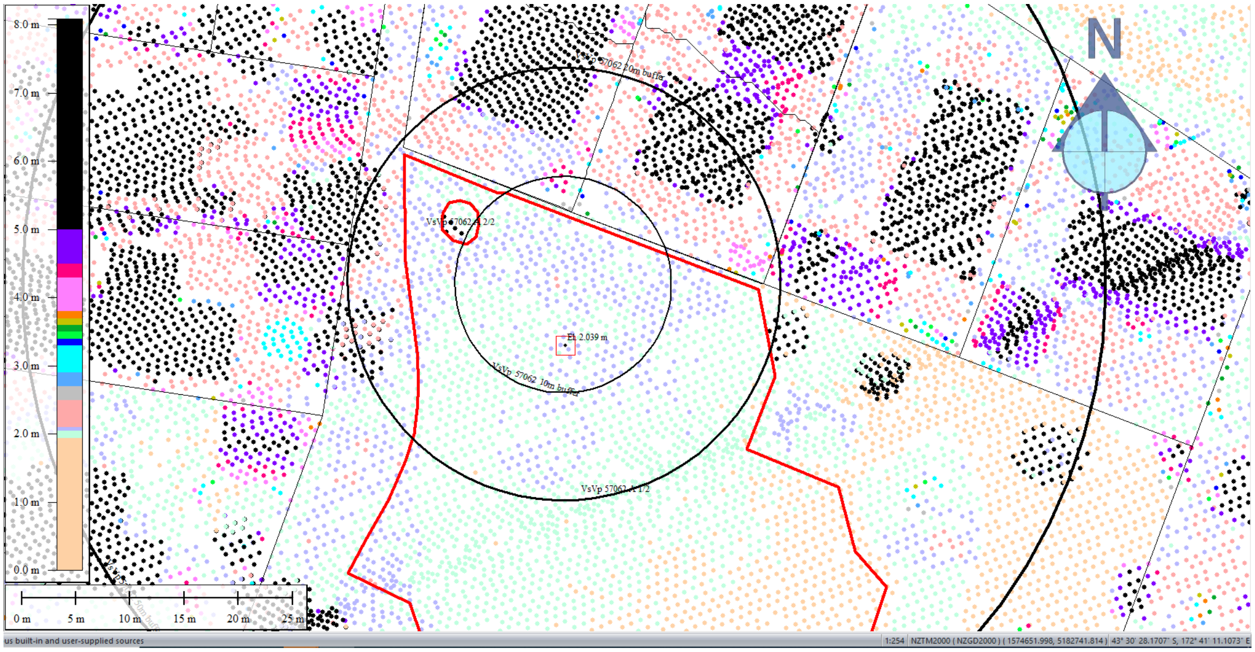

Figure 48: Ground surface elevation averaged over 20-m buffer for Sep 5, 2010 LiDAR survey.

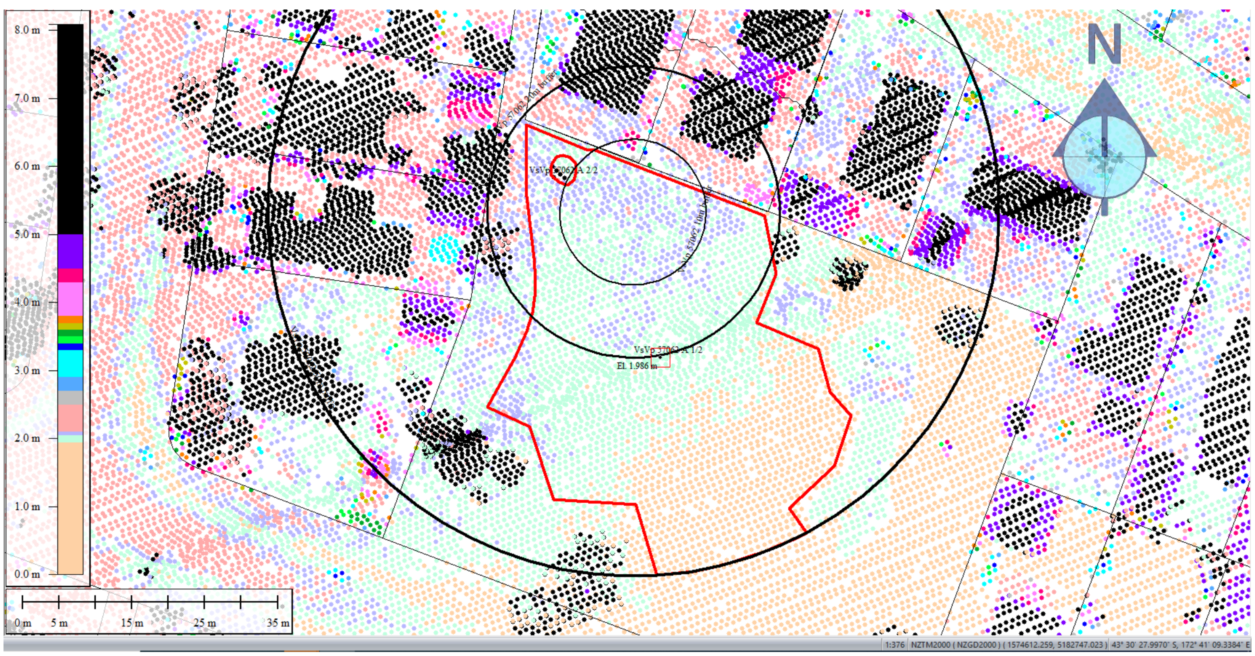

Figure 49: Ground surface elevation averaged over 50-m buffer for Sep 5, 2010 LiDAR survey.

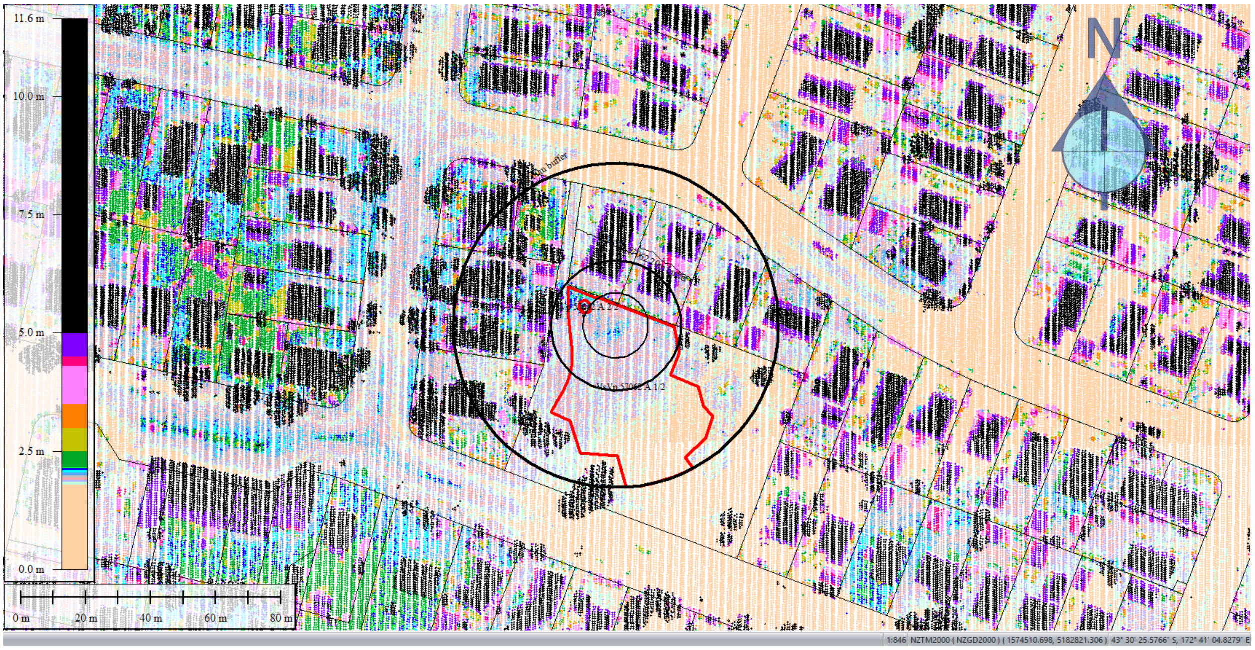

Figure 50: Mar 2011 LiDAR survey.

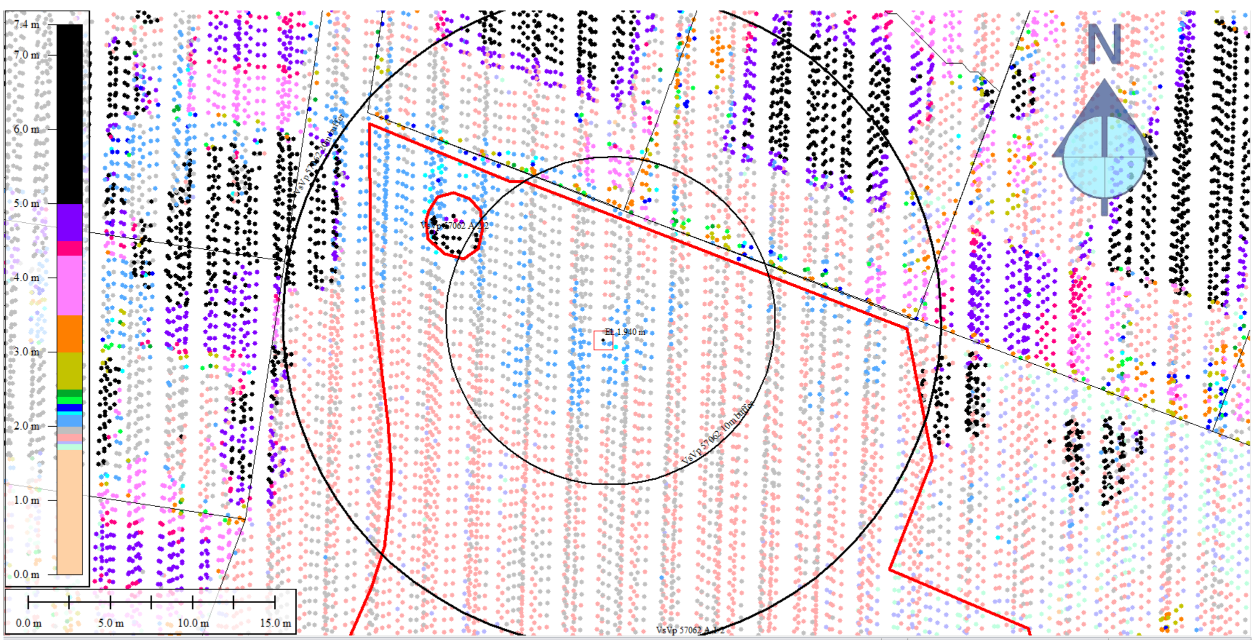

Figure 51: Ground surface elevation averaged over 10-m buffer for Mar 2011 LiDAR survey.

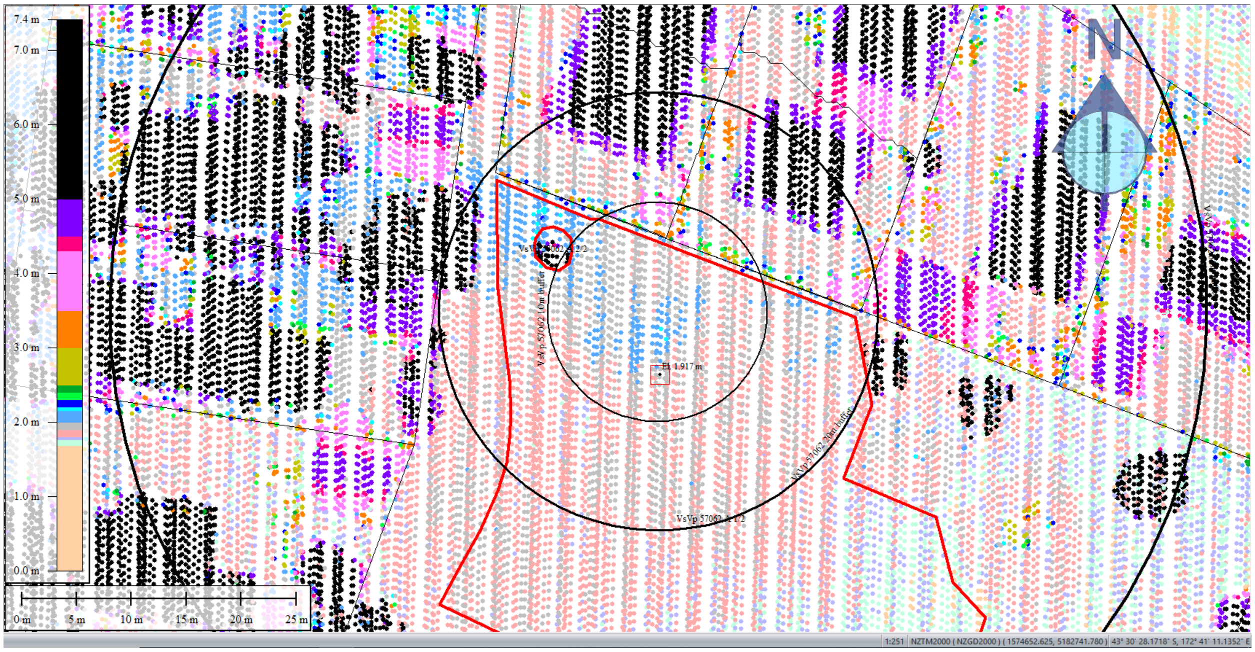

Figure 52: Ground surface elevation averaged over 20-m buffer for Mar 2011 LiDAR survey.

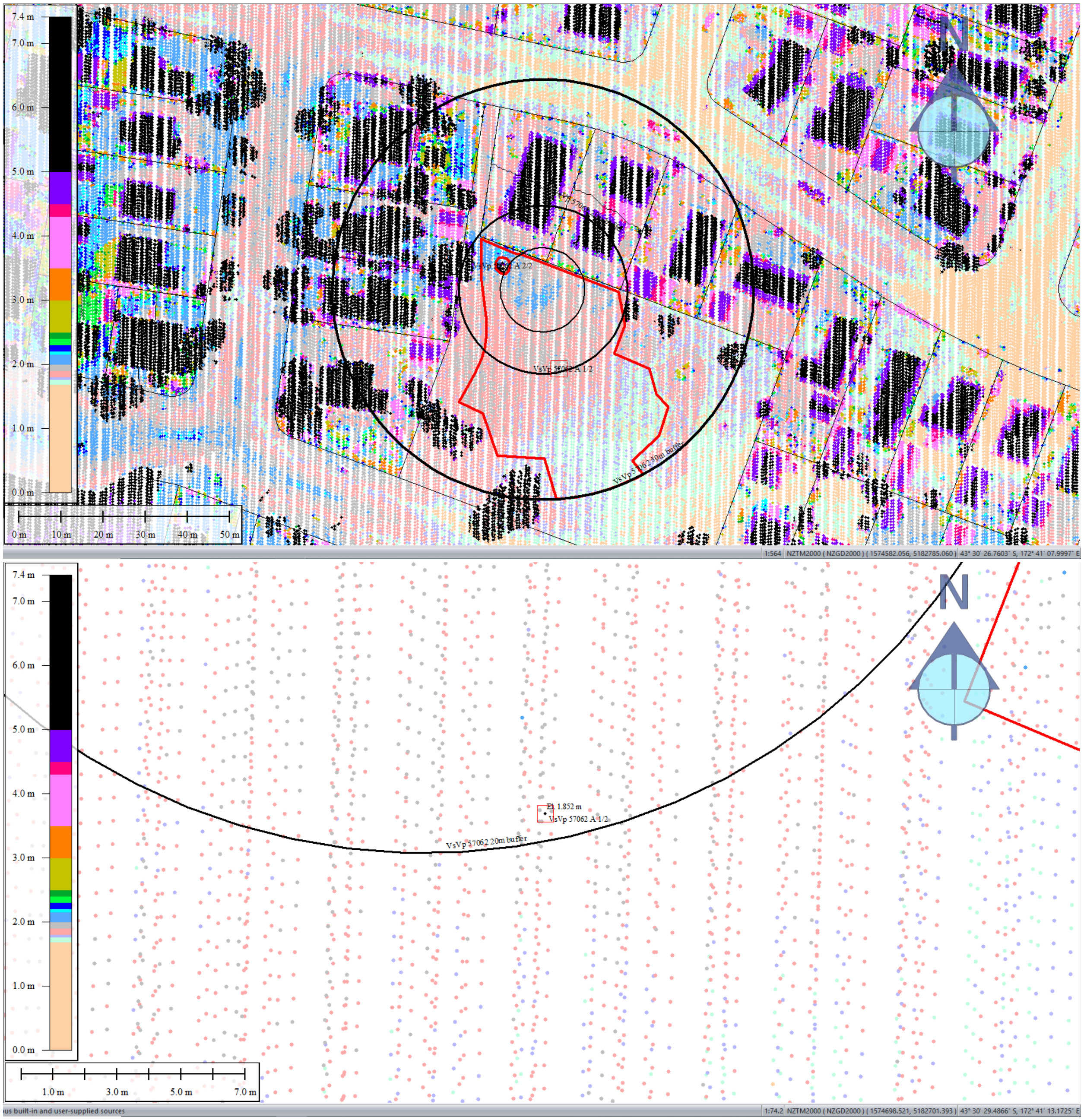

Figure 53: Ground surface elevation averaged over 50-m buffer for Mar 2011 LiDAR survey.

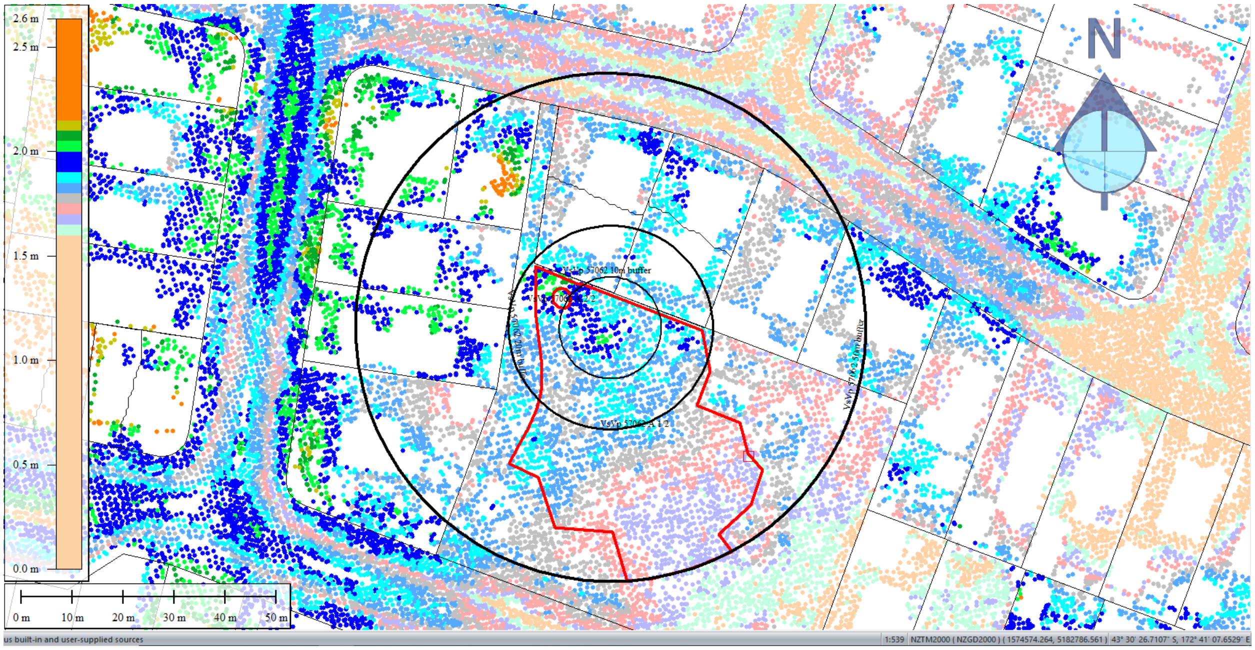

Figure 54: May 2011 LiDAR survey.

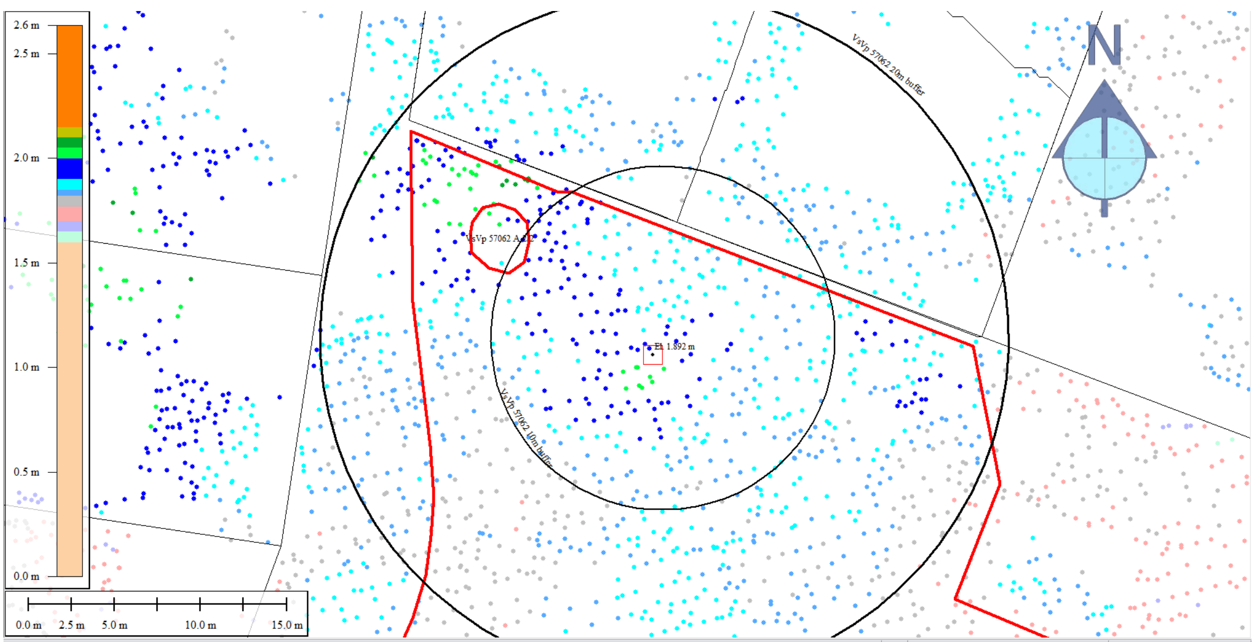

Figure 55: Ground surface elevation averaged over 10-m buffer for May 2011 LiDAR survey.

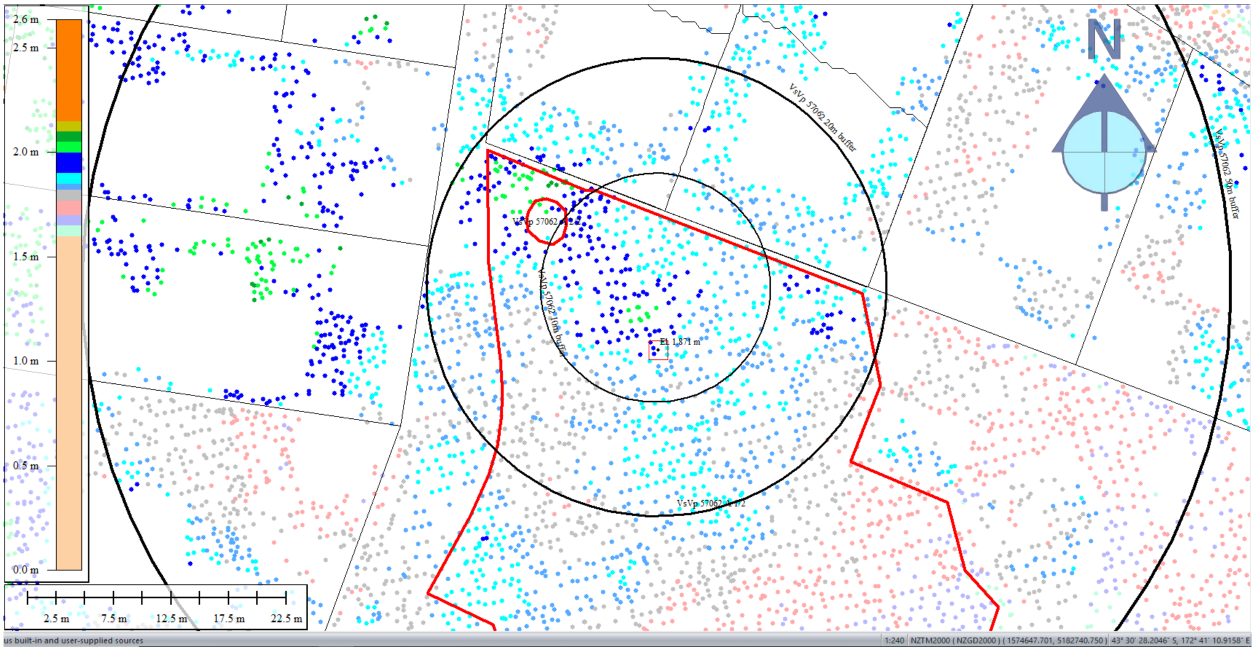

Figure 56: Ground surface elevation averaged over 20-m buffer for May 2011 LiDAR survey.

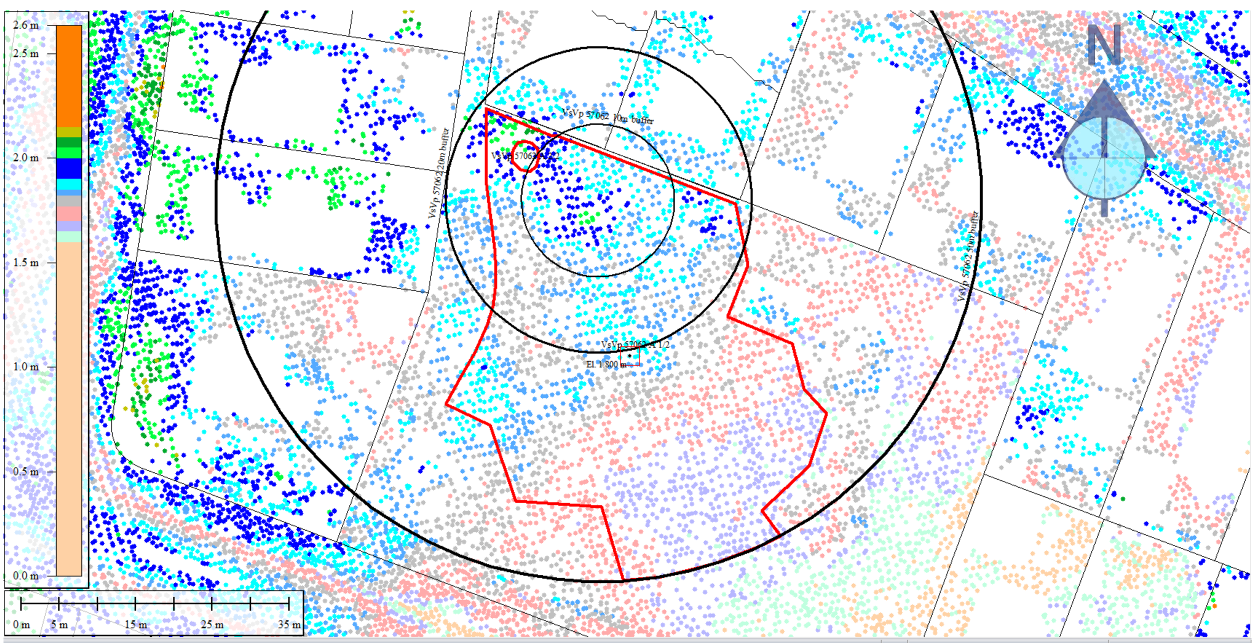

Figure 57: Ground surface elevation averaged over 50-m buffer for May 2011 LiDAR survey.

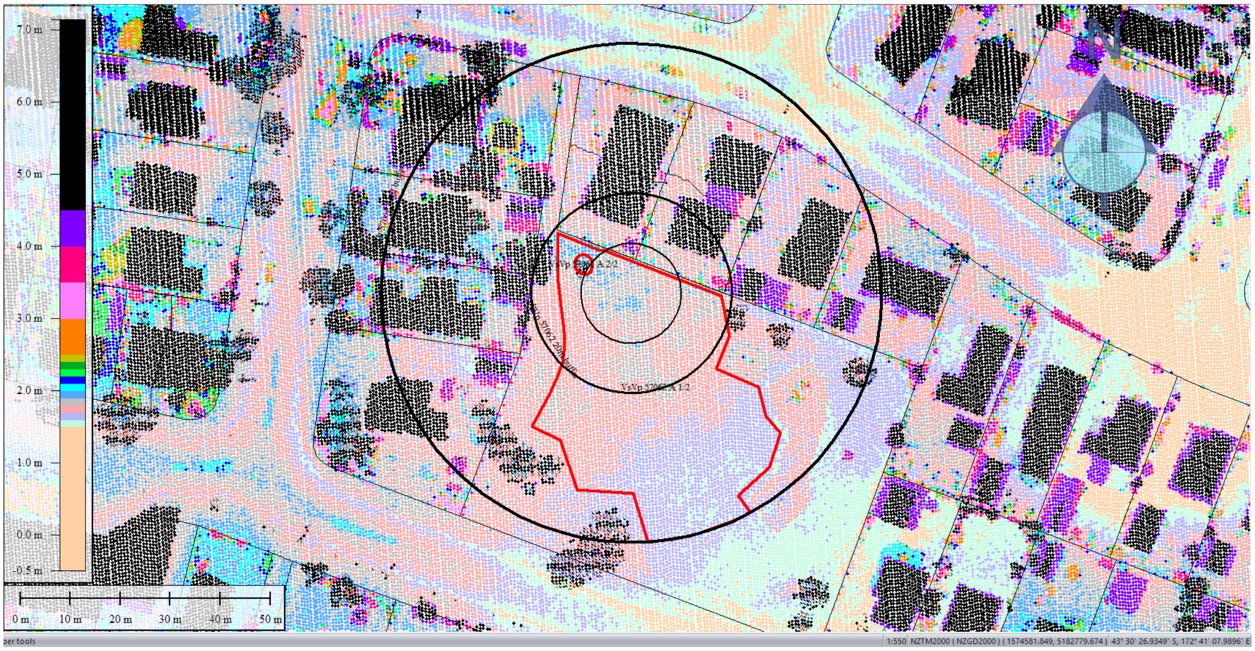

Figure 58: Sep 2011 LiDAR survey.

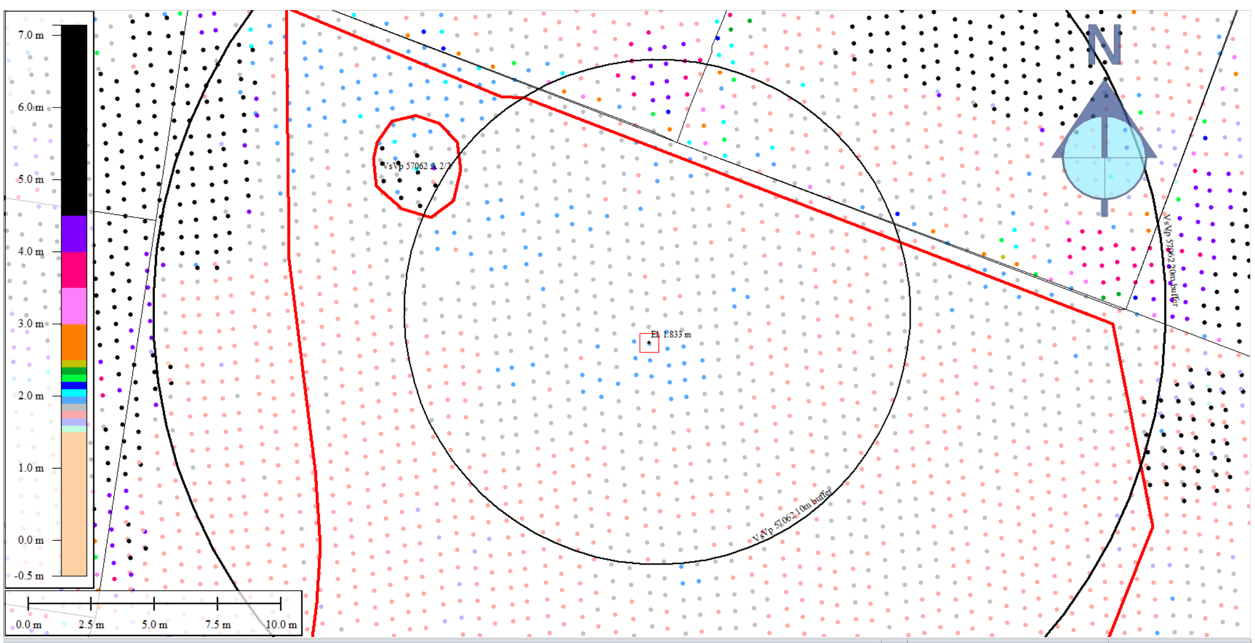

Figure 59: Ground surface elevation averaged over 10-m buffer for Sep 2011 LiDAR survey.

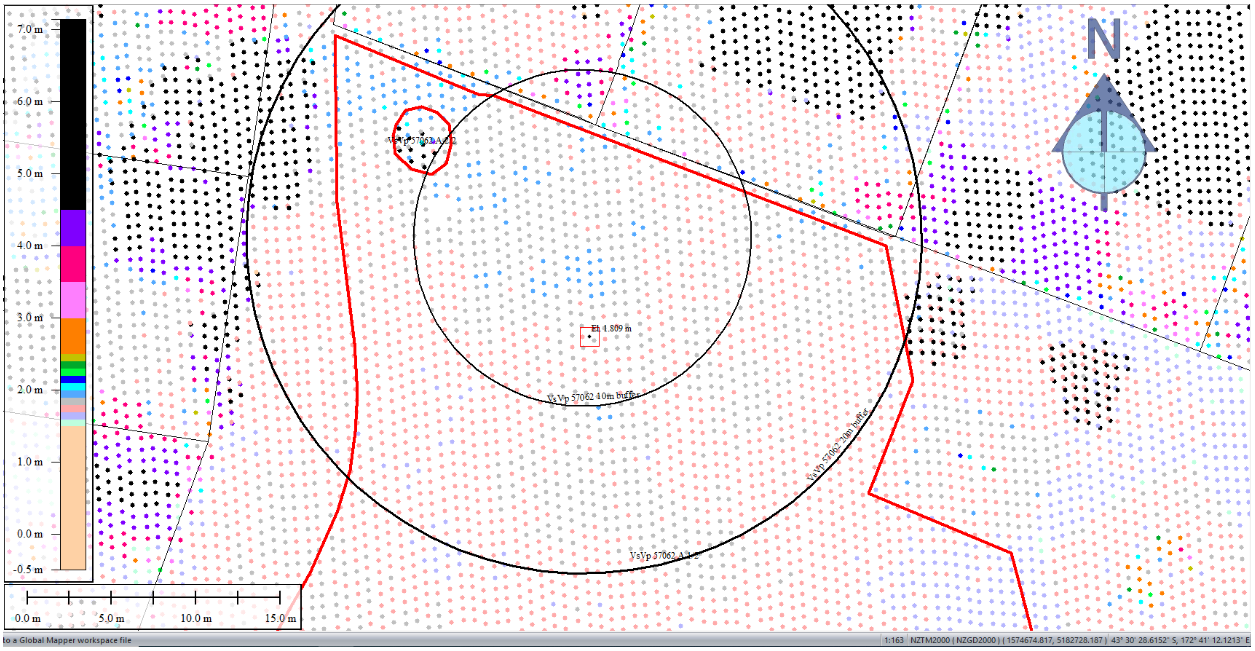

Figure 60: Ground surface elevation averaged over 20-m buffer for Sep 2011 LiDAR survey.

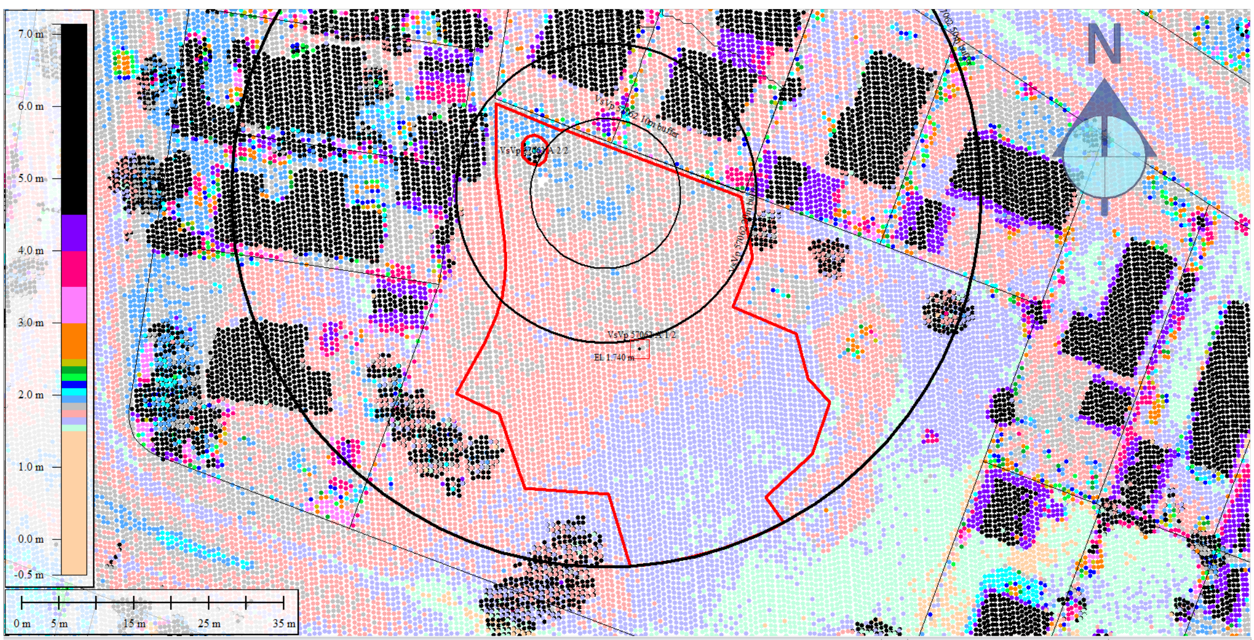

Figure 61: Ground surface elevation averaged over 50-m buffer for Sep 2011 LiDAR survey.

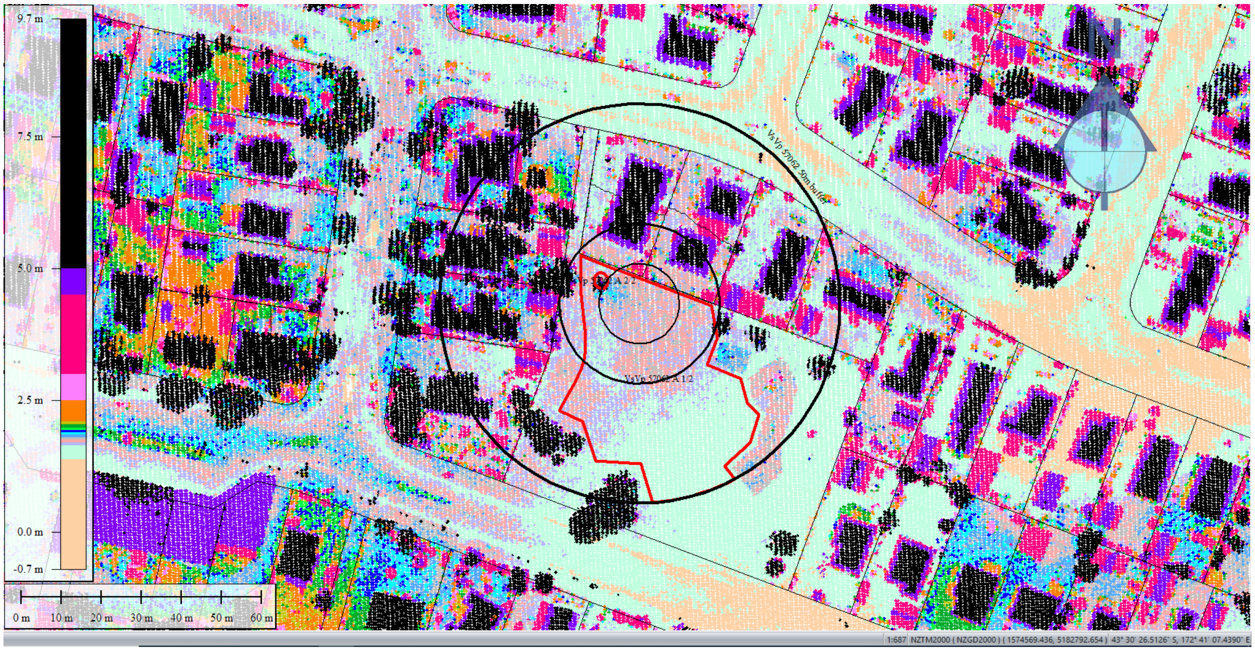

Figure 62: Feb 2012 LiDAR survey.

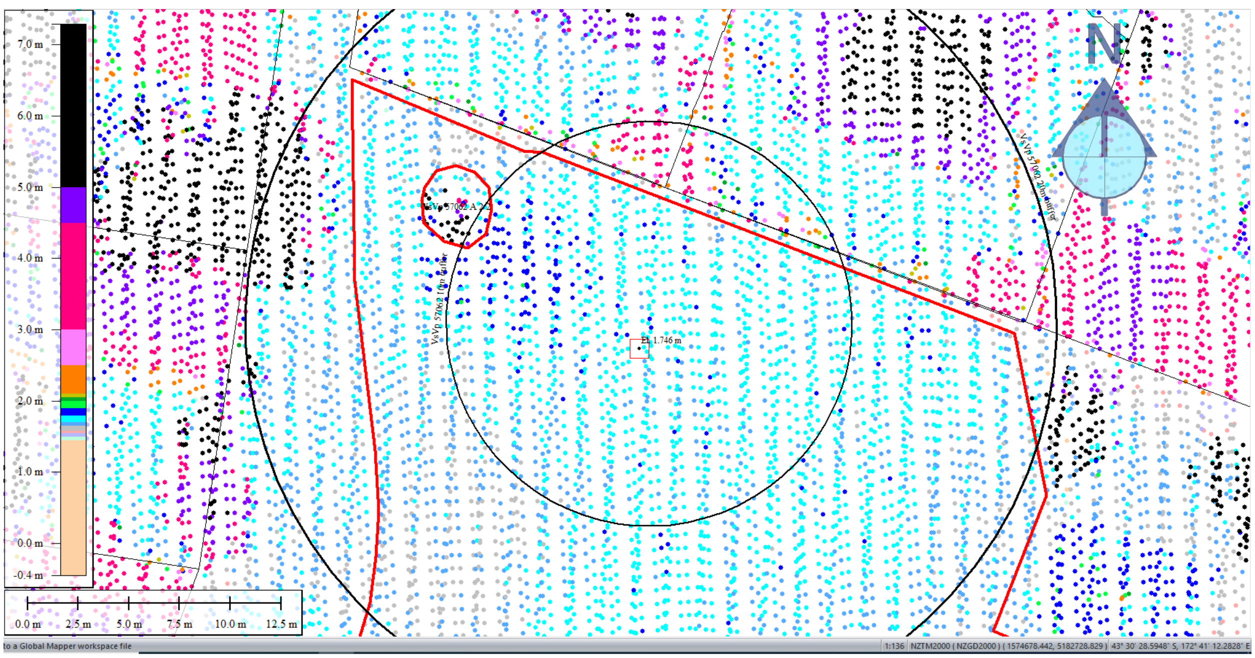

Figure 63: Ground surface elevation averaged over 10-m buffer for Feb 2012 LiDAR survey.

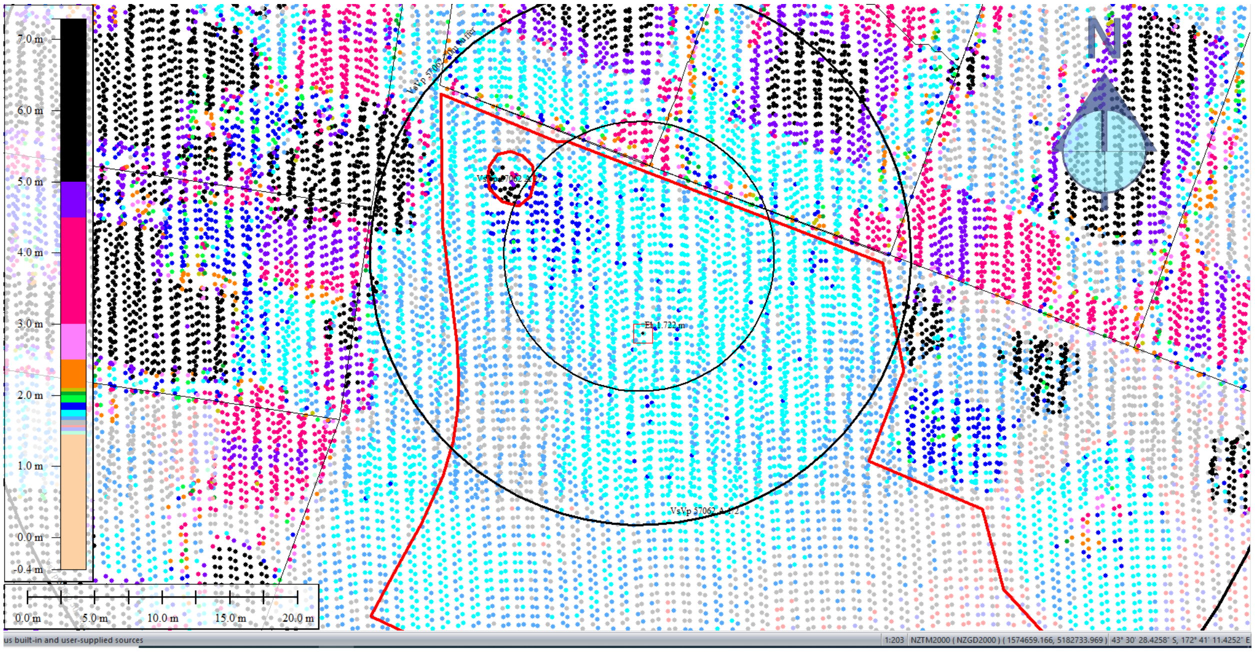

Figure 64: Ground surface elevation averaged over 20-m buffer for Feb 2012 LiDAR survey.

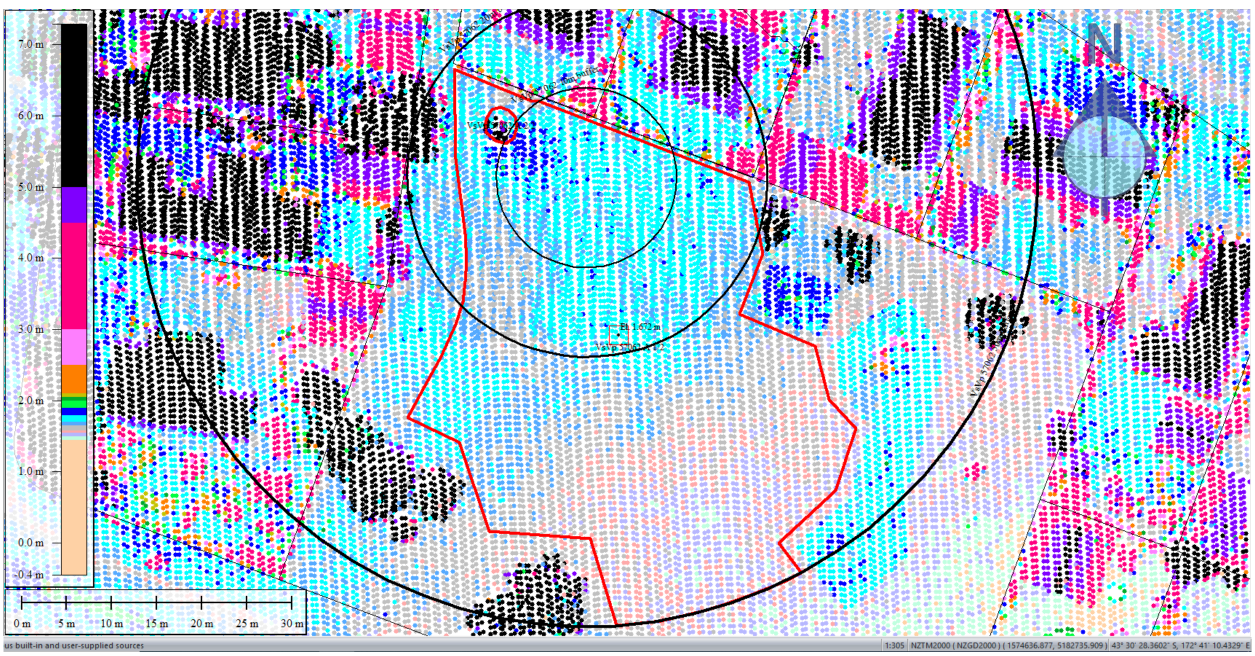

Figure 65: Ground surface elevation averaged over 50-m buffer for Feb 2012 LiDAR survey.

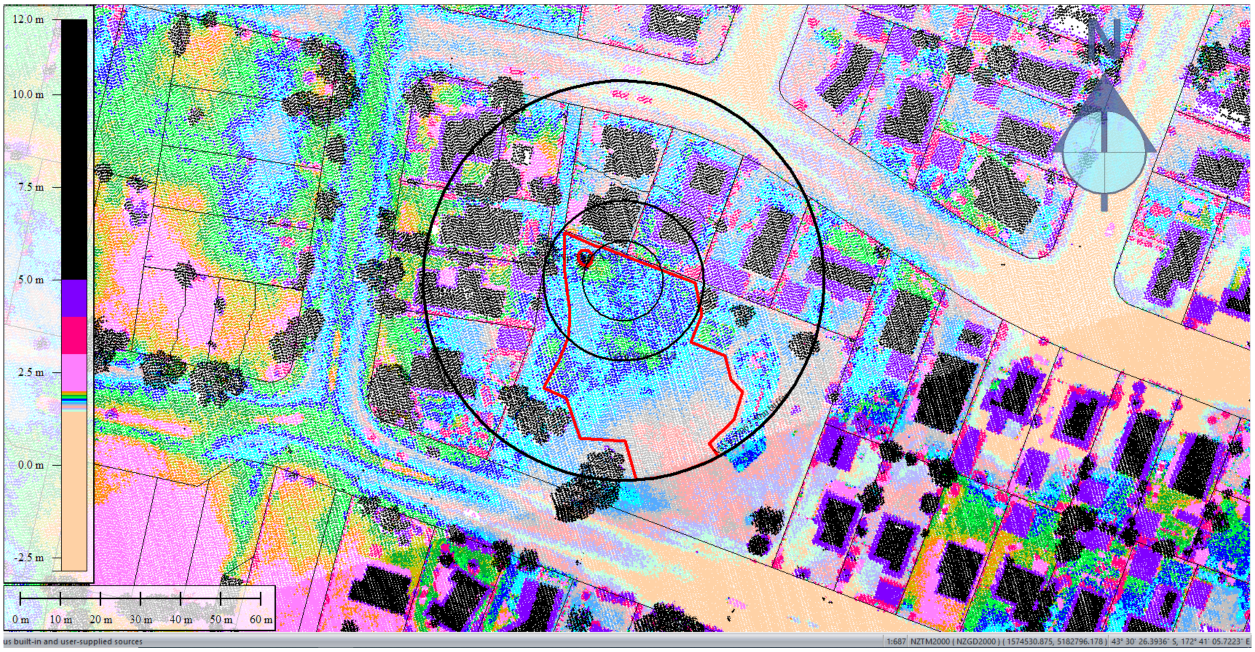

Figure 66: Oct 2015 LiDAR survey.

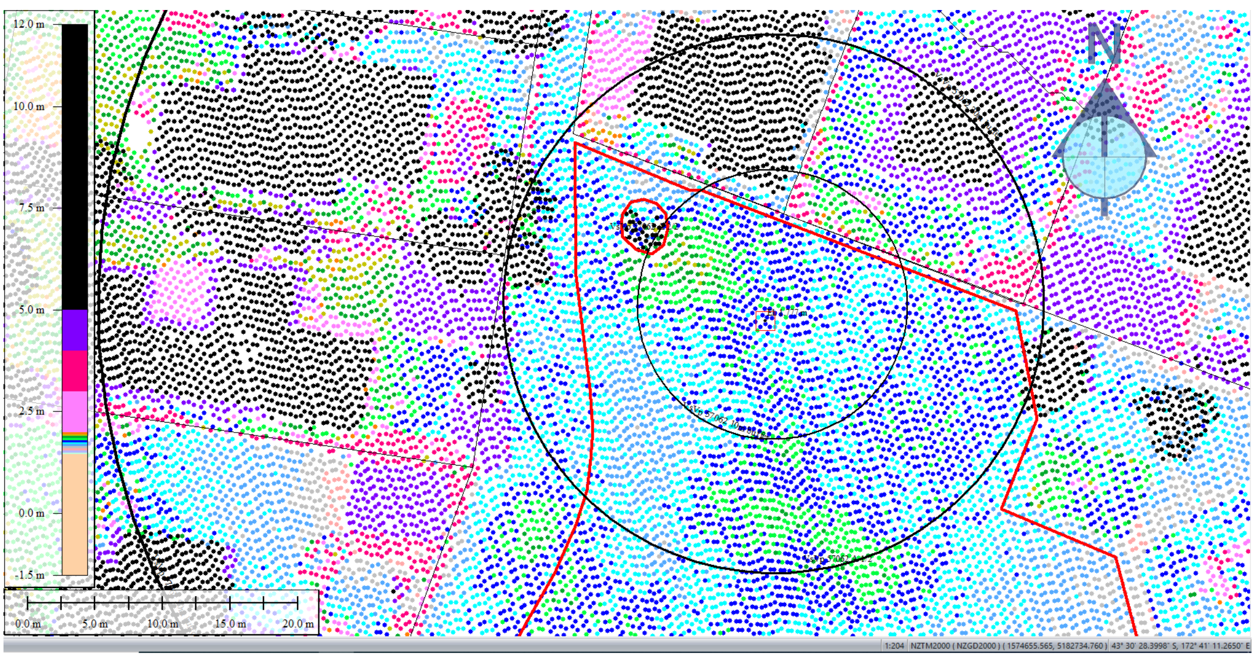

Figure 67: Ground surface elevation averaged over 10-m buffer for Oct 2015 LiDAR survey.

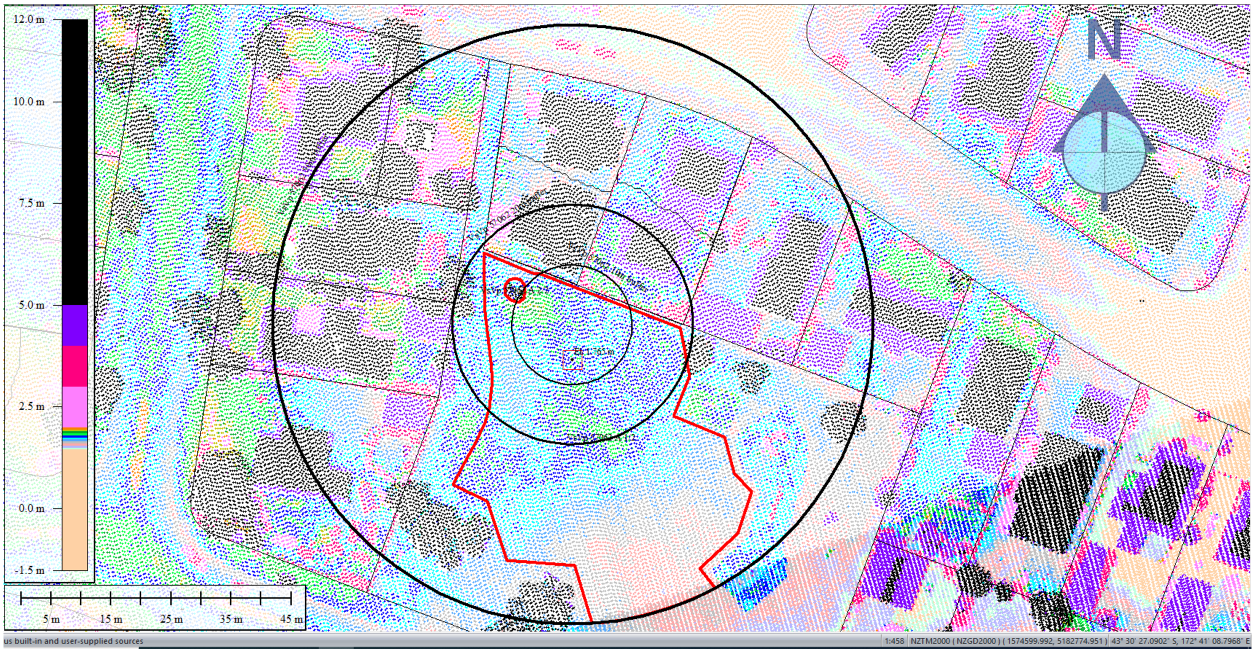

Figure 68: Ground surface elevation averaged over 20-m buffer for Oct 2015 LiDAR survey.

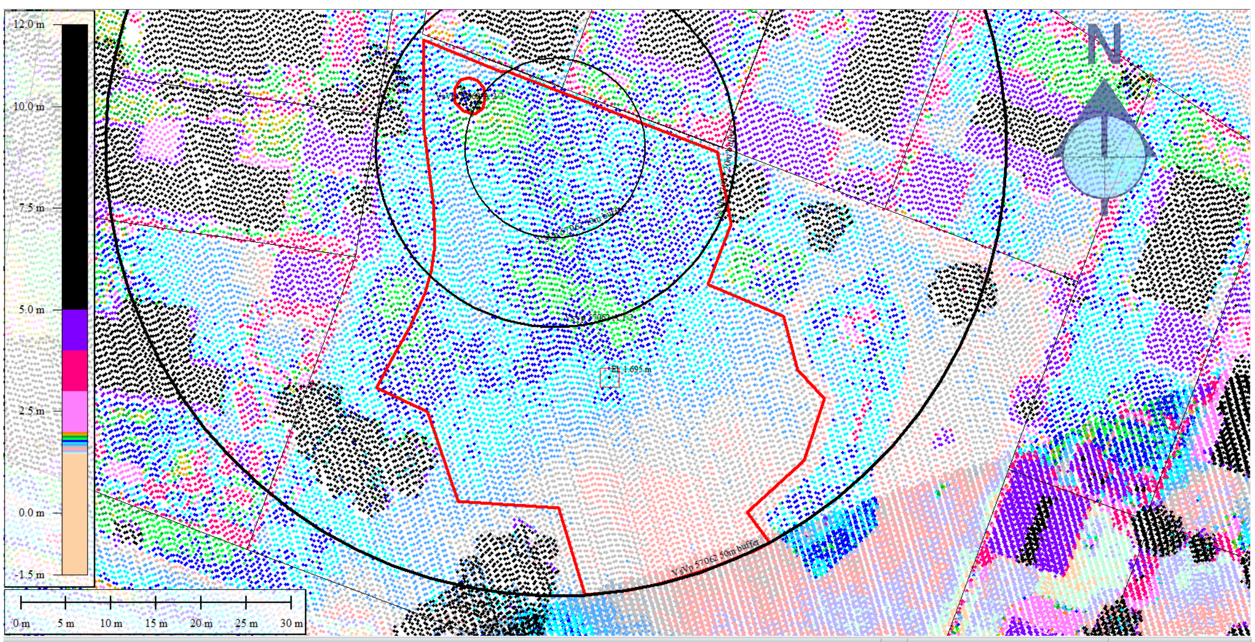

Figure 69: Ground surface elevation averaged over 50-m buffer for Oct 2015 LiDAR survey.

Figure 70: Absence of ejecta for Sep-10 EQ.

Figure 71: Ejecta outline for Feb-11 EQ.

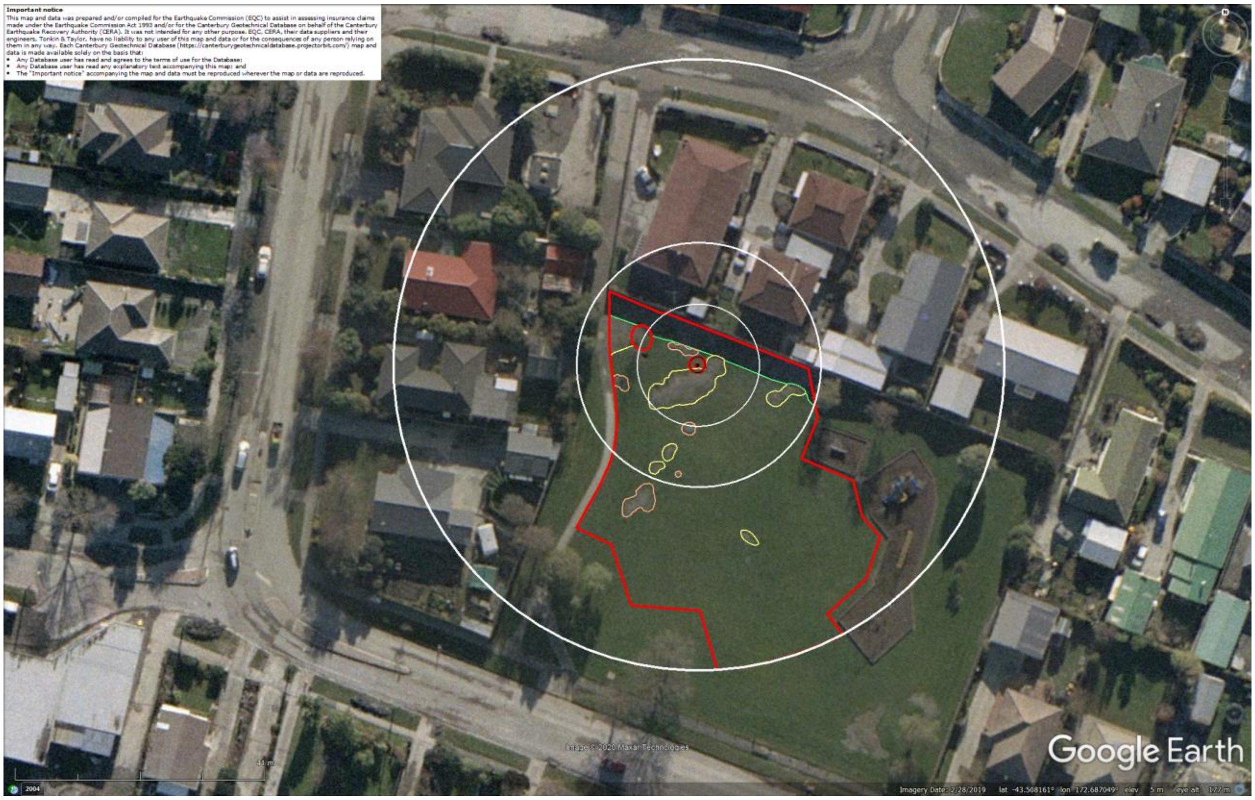

Figure 72: Ejecta outline for Jun-11 EQ.

Figure 73: No indications of fresh ejecta at the site for Dec-11 EQ.

Figure 74: Evidence of ejecta at the property within the 50-m buffer (the photographs were acquired on 08-08-2011).

Figure 75: PGA for Sep-10 EQ (st. dev. = 0.300-0.325 ln units).

Figure 76: PGA for Feb-11 EQ (st. dev. = 0.325-0.350 ln units).

Figure 77: PGA for Jun-11 EQ (st. dev. = 0.325-0.350 ln units).

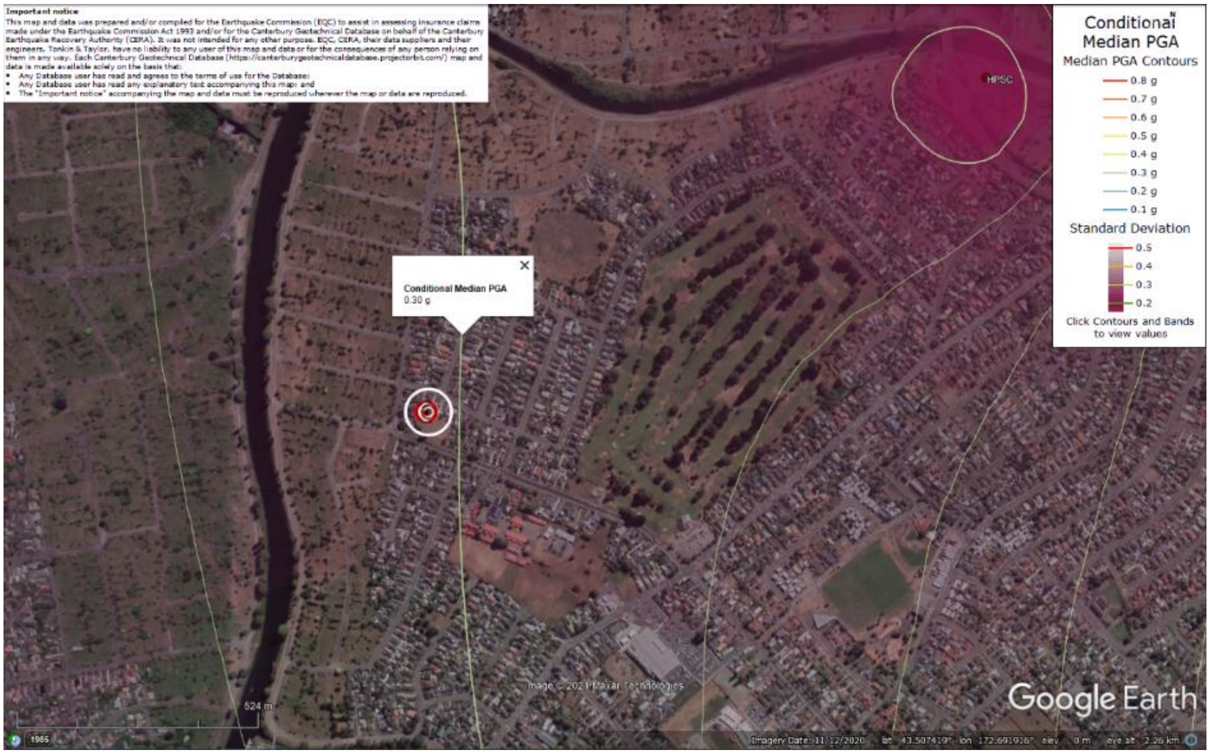

Figure 78: PGA for Dec-11 EQ (st. dev. = 0.350-0.375 ln units).

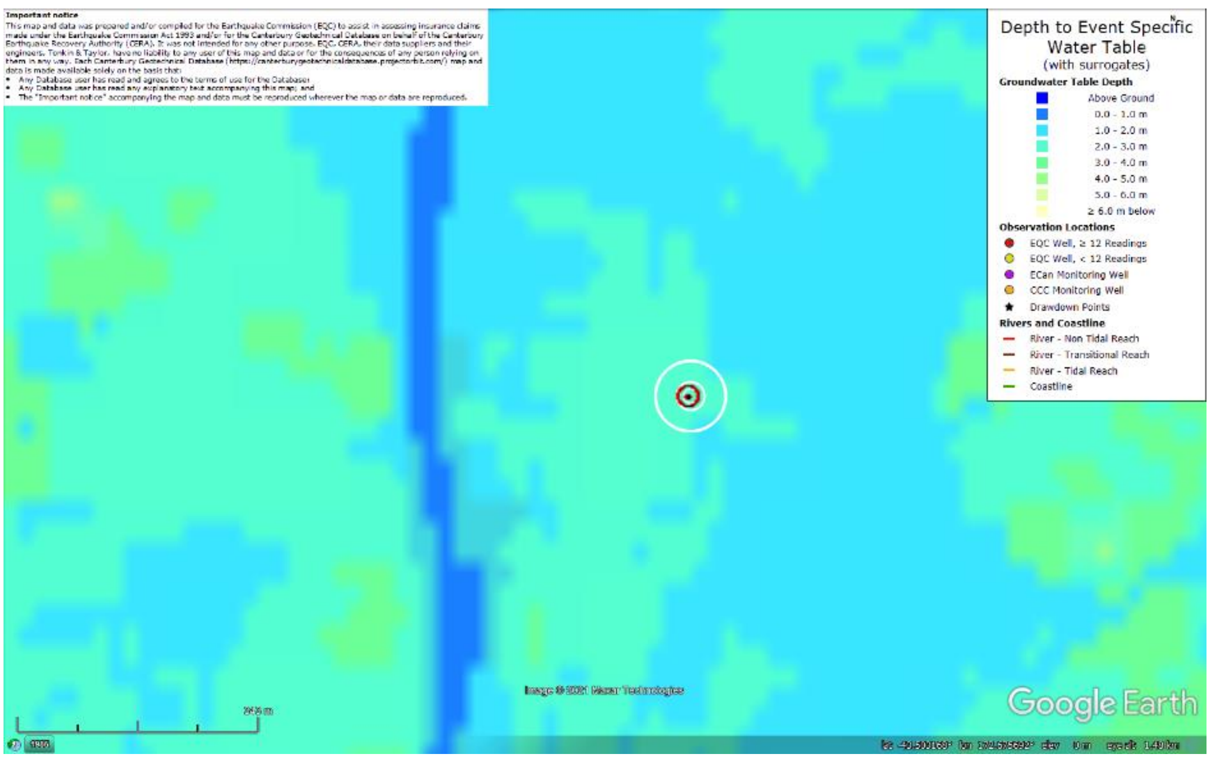

Figure 79: Depth to groundwater table for Sep-10 EQ.

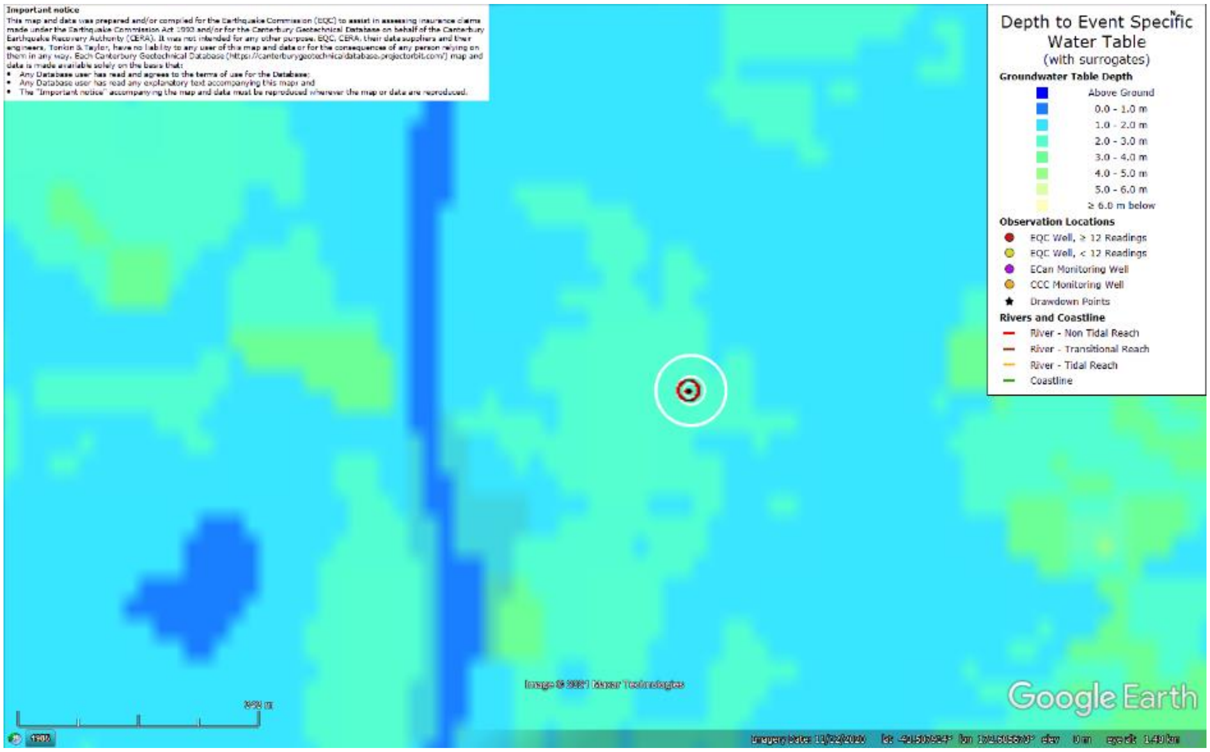

Figure 80: Depth to groundwater table for Feb-11 EQ.

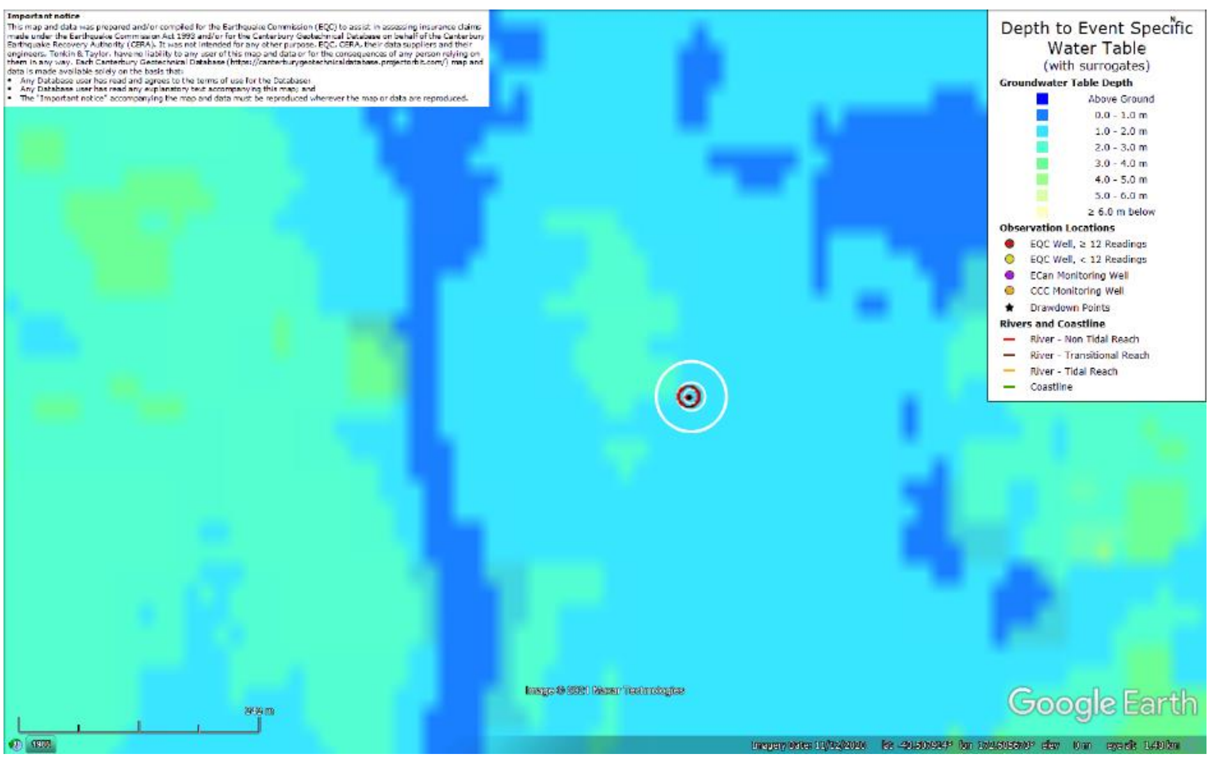

Figure 81: Depth to groundwater table for Jun-11 EQ.

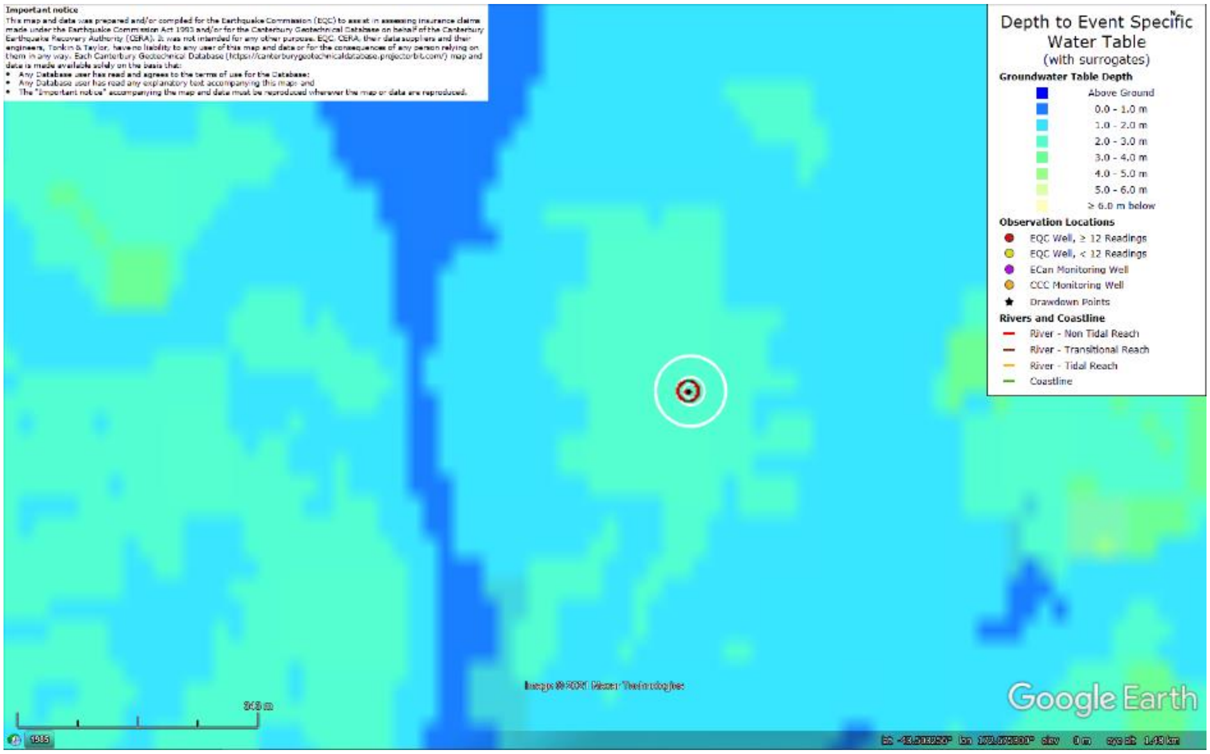

Figure 82: Depth to groundwater table for Dec-11 EQ.

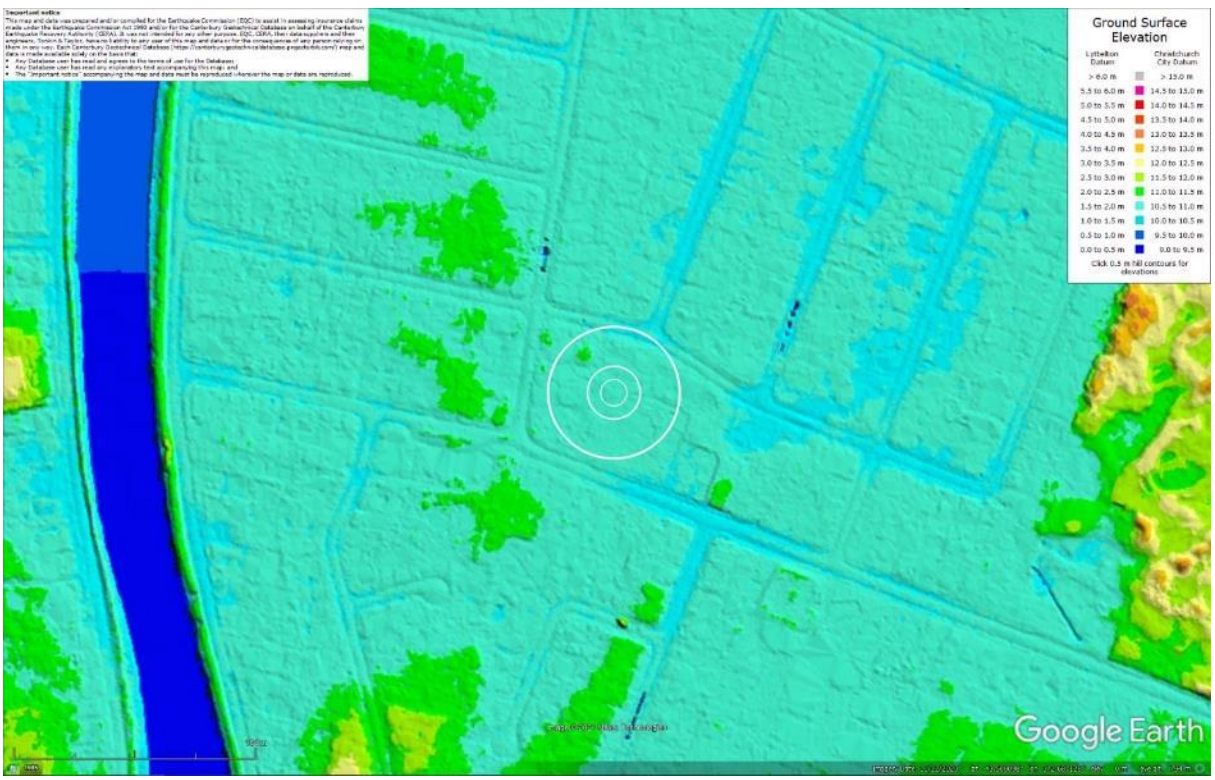

Figure 83: Ground surface elevation according to the Sep-11 LiDAR survey.

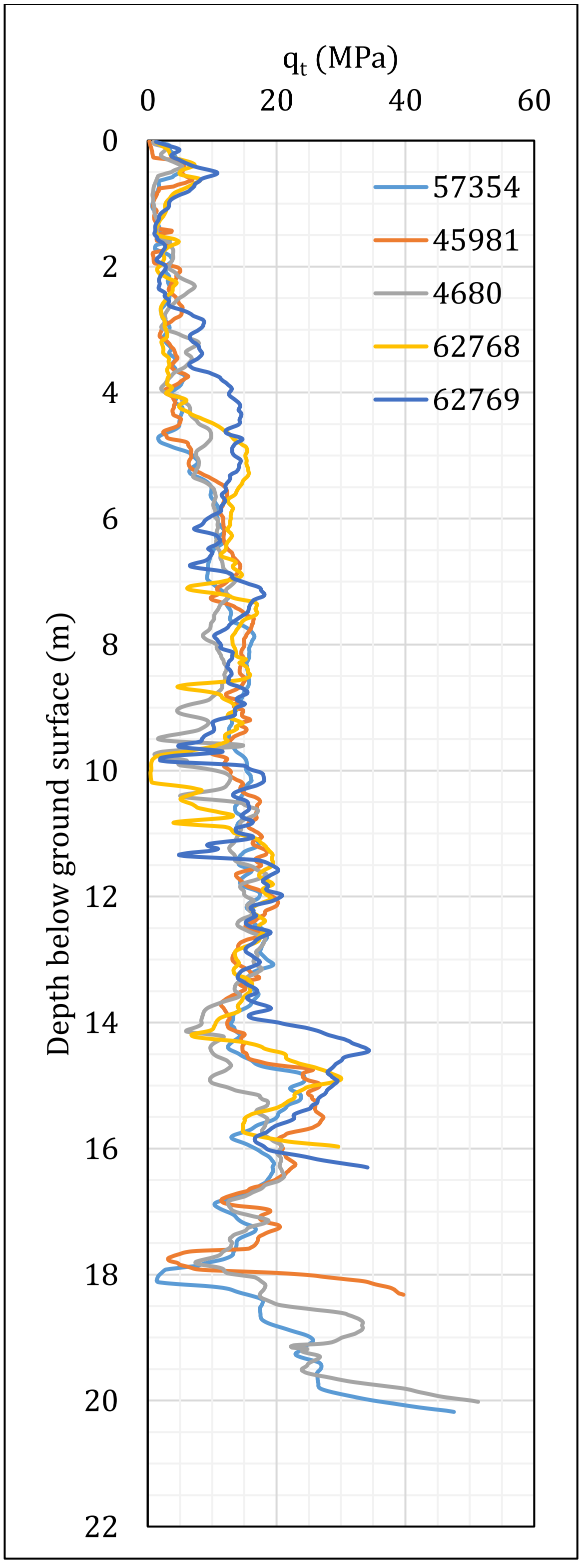

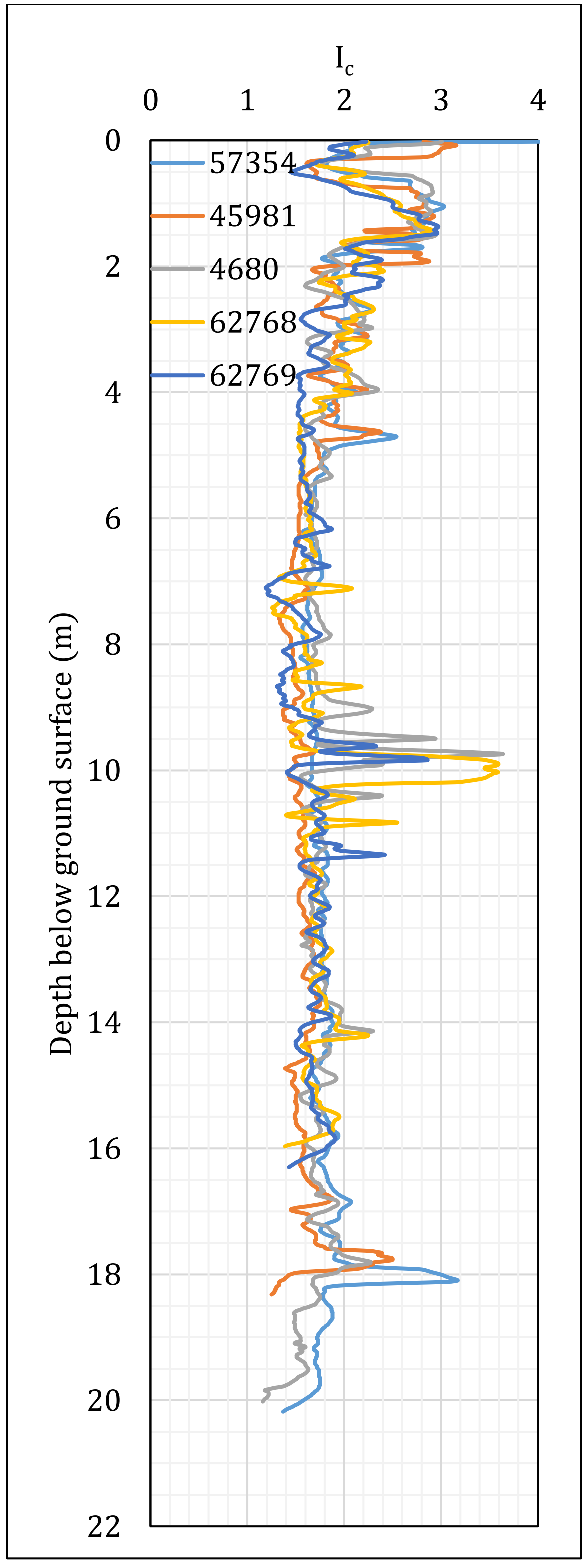

Figure 84: q_t and I_c profiles.

Note 8: The selection of CPTs for the area considered for settlement assessment (Figure 1) is based on the proximity of the CPTs to the considered areas. In accordance with that, the following table shows CPTs that were used for the volumetric settlement analysis in *Cliq v.3.0.3.2*, a CPT soil liquefaction software developed by GeoLogismiki. (The average volumetric settlements were reported in Table 8.)

Table 12: CPT profiles used in volumetric settlement analysis for areas selected for settlement assessment.

CPT ID No.	10-m buffer	20-m buffer	50-m buffer
57354 (56732)	✓	✓	✓
62768 (60919)		✓	✓
45981		✓	✓
4680		✓	✓
62769 (60920)			✓

Note: CPT 57354 was used to calculate the volumetric settlement at depths between 16 m and 20 m for CPTs 62768 and 62769 and depths between 18 m and 20 m for CPT 45981.

Table 13: CPT-based results.

EQ Event	Parameter	CPT ID 57354	45981	4680	62768	62769	$\Delta_{16m-20m}$	$\Delta_{18m-20m}$
Sep-10	S_{V1D} (mm)	7	14	11	18	8	2	1
	LSN	1	2	1	3	1	0	0
	LPI	0	0	0	0	0	0	0
	LPI_{ish}	0	0	0	0	0	--	--
	$D_{FS<1}$ (m)	undet.	undet.	undet.	undet.	undet.	--	--
Feb-11	S_{V1D} (mm)	93	121	134	94	66	5	2
	LSN	22	23	22	21	13	0	0
	LPI	8	10	9	9	5	0	0
	LPI_{ish}	5	5	4	6	0	--	--
	$D_{FS<1}$ (m)	2.22	2.21	2.60	2.22	2.22	--	--
Jun-11	S_{V1D} (mm)	32	49	39	54	24	2	1
	LSN	8	10	7	12	5	0	0
	LPI	1	1	1	2	1	0	0
	LPI_{ish}	0	0	0	0	0	--	--
	$D_{FS<1}$ (m)	2.68	2.94	3.78	3.08	6.58	--	--
Dec-11	S_{V1D} (mm)	30	52	46	51	22	3	1
	LSN	7	9	7	10	3	0	0
	LPI	1	2	1	3	1	0	0
	LPI_{ish}	0	0	0	0	0	--	--
	$D_{FS<1}$ (m)	2.68	2.94	3.78	3.08	6.46	--	--

Notes: $D_{FS<1}$ = Depth to the first liquefiable layer (FS_L<1) that is at least 200-mm thick, as determined by the Boulanger and Idriss (2016) liquefaction-triggering procedure (P_L=50%, C_{FC}=0.13, and $I_{c,cutoff}$ =2.6), and exported from *Cliq v.3.0.3.2*; undet. = the specified soil layer was not detected; $\Delta_{16m-20m}$ and $\Delta_{18m-20m}$ indicate the amount of S_{V1D}, LSN, and LPI added to CPTs 62768 and 62769 and CPT 45981, respectively.

Note 9: Based on the borehole log (BH 57217, Figure 1), the groundwater table is at a depth of 0.9 m below the ground surface. The ground subsurface profile consists of (1) organic silt and fine to medium sand, SP, with organics to a depth of 0.7 m, (2) silt, ML, of the Christchurch formation to a depth of 1.85 m, and (3) fine to medium sand, SP, of the Christchurch formation to a depth of 15.65 m (the end of the borehole). The nearby borehole (BH 9477) suggests that the SP stratum extends to a 20-m depth.

Note 10: The ejecta-induced free-field settlement provided in Table 11 is an areal average settlement due to ejecta, which is based on the total settlement assessment area, A_T (provided in Table 9 and repeated in Table 14). However, the considered area was not always covered completely with ejecta; thus, it is important to provide the localized ejecta-induced settlement, too. The localized settlement due to ejecta is estimated using photographic evidence only as

$$S_{E,P\_localized} = \frac{V_E}{A_E}$$

where V_E is the total volume of ejecta within A_T and A_E is the total coverage area of ejecta within A_T. Please note that the areal ejecta-induced settlement provided in Table 14 as S_{E,P_areal} is the same as $S_{E,P}$ in Table 11, which was estimated as

$$S_{E,P\_areal} = S_{E,P} = \frac{V_E}{A_T}$$

where V_E is the total volume of ejecta within A_T and A_T is the total settlement assessment area.

Table 14a: Areal and localized ejecta-induced settlement estimates for Patch A (10-m buffer) based on photographic evidence.

Earthquake Event	A_T (m^2)	A_E (m^2)	V_E (m^3)	S_{E,P_areal} (mm)	$S_{E,P\_localized}$ (mm)
Sep-10	266	0	0	0	0
Feb-11	259	108	9.4-18.0	55±15	125±40
Jun-11	198	64.9	3.3-6.5	25±10	75±25
Dec-11	266	0	0	0	0

Notes: S_{E,P_areal} = $S_{E,P}$ reported in Table 11 = areal ejecta-induced settlement; $S_{E,P\_localized}$ = localized ejecta-induced settlement; A_T = total settlement assessment area; V_E = total volume of ejecta within A_T; A_E = total area of ejecta within A_T; The estimates of both areal and localized ejecta-induced settlement are rounded to the nearest 5; Final plus/minus values are also rounded to the nearest 5.

Table 14b: Areal and localized ejecta-induced settlement estimates for Patch A (20-m buffer) based on photographic evidence.

Earthquake Event	A_T (m^2)	A_E (m^2)	V_E (m^3)	S_{E,P_areal} (mm)	$S_{E,P\_localized}$ (mm)
Sep-10	729	0	0	0	0
Feb-11	721	229	19.6-37.9	40±15	125±40
Jun-11	598	114	5.7-11.4	10±5	75±25
Dec-11	729	0	0	0	0

Notes: S_{E,P_areal} = $S_{E,P}$ reported in Table 11 = areal ejecta-induced settlement; $S_{E,P\_localized}$ = localized ejecta-induced settlement; A_T = total settlement assessment area; V_E = total volume of ejecta within A_T; A_E = total area of ejecta within A_T; The estimates of both areal and localized ejecta-induced settlement are rounded to the nearest 5; Final plus/minus values are also rounded to the nearest 5.

Table 14c: Areal and localized ejecta-induced settlement estimates for Patch A (50-m buffer) based on photographic evidence.

Earthquake Event	A_T (m^2)	A_E (m^2)	V_E (m^3)	S_{E,P_areal} (mm)	$S_{E,P\_localized}$ (mm)
Sep-10	1839	0	0	0	0
Feb-11	1831	244	20.7-40.2	15±5	125±40
Jun-11	1708	135	6.8-13.5	5±5	75±25
Dec-11	1839	0	0	0	0

Notes: S_{E,P_areal} = $S_{E,P}$ reported in Table 11 = areal ejecta-induced settlement; $S_{E,P\_localized}$ = localized ejecta-induced settlement; A_T = total settlement assessment area; V_E = total volume of ejecta within A_T; A_E = total area of ejecta within A_T; The estimates of both areal and localized ejecta-induced settlement are rounded to the nearest 5; Final plus/minus values are also rounded to the nearest 5.

Summary 2:

The best estimate of the localized ejecta-induced free-field ground settlement at the Avondale Playground site for the SEP 2010, FEB 2011, JUN 2011, and DEC 2011 earthquake is 0 mm, 125±40 mm, 75±25 mm, and 0 mm, respectively.